Neuroscience Research 70 (2011) 442–448

Contents lists available at ScienceDirect

Neuroscience Research

journal homepage: www.elsevier.com/locate/neures

LORETA analysis of three-dimensional distribution of delta band activity in schizophrenia: Relation to negative symptoms

Toru Itoh[a], Tomiki Sumiyoshi[a,b,*], Yuko Higuchi[a], Michio Suzuki[a,b], Yasuhiro Kawasaki[c]

[a] Department of Neuropsychiatry, University of Toyama Graduate School of Medicine and Pharmaceutical Sciences, Toyama, Japan
[b] Core Research for Evolutional Science and Technology, Japan Science and Technology Corporation, Tokyo, Japan
[c] Department of Neuropsychiatry, Kanazawa Medical University, Uchinada-machi, Ishikawa, Japan

ARTICLE INFO

Article history:
Received 18 March 2011
Received in revised form 1 May 2011
Accepted 2 May 2011
Available online 27 May 2011

Keywords:
Schizophrenia
Electroencephalography
LORETA
Delta band activity
Negative symptoms
Prefrontal cortex

ABSTRACT

We sought to determine if altered electroencephalography (EEG) activities, such as delta band activity, in specific brain regions are associated with psychotic symptoms. Data were obtained from 17 neuroleptic-naive patients with schizophrenia and age- and sex-matched 17 healthy control subjects. Low Resolution Brain Electromagnetic Tomography (LORETA) was used to generate current source density images of delta, theta, alpha, and beta activities. Localization of the difference in EEG activity between the two groups was assessed by voxel-by-voxel non-paired *t*-test of the LORETA images. Spearman's correlation coefficient was obtained to relate LORETA values of EEG current density in brain regions showing a significant between-group difference and psychopathology scores. Delta band activity, represented by LORETA current density, was greater for patients in the following areas; the left inferior temporal gyrus, right middle frontal gyrus, right superior frontal gyrus, right inferior frontal gyrus, and right parahippocampal gyrus. LORETA values for delta band activity in the above five brain regions were negatively correlated with negative, but not positive symptoms. The results of this study suggest the role for electrophysiological changes in some of the brain regions, e.g. prefrontal cortex, in the manifestation of negative symptoms.

1. Introduction

Schizophrenia is a relatively common and often debilitating neuropsychiatric disorder that develops after puberty with prevalence being approximately 0.85% throughout life. Its symptoms include positive symptoms (e.g. delusions, hallucinations, and thought disorders), negative symptoms (e.g. affective flattening, and poverty of speech), and cognitive deficits, such as impairment of memory and attention (Crow, 1980; Sumiyoshi et al., 2000).

Imaging studies have suggested functional deviations in various brain areas, especially, prefrontal cortex (Cleghorn et al., 1989; Andreasen et al., 1992, 1997; Parellada et al., 1994; Sabri et al., 1997) in subjects with schizophrenia.

Although some brain imaging methods based on blood flow or metabolism, e.g. fMRI and PET, are associated with high spatial resolution, they may not appropriately differentiate functional excitation and inhibition of neural 38 activity (Pascual-Marqui et al., 1999).

Electroencephalography (EEG) offers information with high time resolution which enables, for example, frequency analysis. However, scalp distributions of EEG power of various frequency bands are generally ambiguous (Pascual-Marqui et al., 1999), and depend on the reference sites used. Therefore, numerical analyses, such as dipole source modeling, are required to obtain precise locations of EEG generators.

Low Resolution Brain Electromagnetic Tomography (LORETA) (Pascual-Marqui et al., 1994; Pascual-Marqui, 1995) has been developed to provide three-dimensional tomography of brain electrical activity, which only requires simple constraints ('smoothness of the solution'), and predetermined knowledge about the putative number of discernible source regions is not necessary. With this method, brain electrical data with high time resolution are transformed into functional imaging of brain activities, since brain electrical activity can be analyzed separately for the different EEG frequency ranges. LORETA has also been widely used for statistical comparisons of intracranial current density distributions between control subjects and patients with neuropsychiatric disorders (Pizzagalli et al., 2001; Flor-Henry et al., 2004).

Abbreviations: EEG, electroencephalography; LORETA, Low Resolution Brain Electromagnetic Tomography; SAPS, the Scale for the Assessment of Positive Symptoms; SANS, the Scales for the Assessment of Negative Symptoms.

* Corresponding author at: Department of Neuropsychiatry, University of Toyama Graduate School of Medicine and Pharmaceutical Sciences, 2630 Sugitani, Toyama 930-0194, Japan. Tel.: +81 76 434 7323; fax: +81 76 434 5030.
E-mail addresses: toru2008@hotmail.co.jp (T. Itoh), tomikisumiyoshi840@hotmail.com (T. Sumiyoshi), yuko.higuchi@auone.jp (Y. Higuchi), suzukim@med.u-toyama.ac.jp (M. Suzuki), kawasaki@kanazawa-med.ac.jp (Y. Kawasaki).

0168-0102/$ – see front matter © 2011 Elsevier Ireland Ltd and the Japan Neuroscience Society. All rights reserved.
doi:10.1016/j.neures.2011.05.003

Table 1
Demographic data of participants.

	Schizophrenia (n = 17)	Healthy controls (n = 17)
Females/Males	6/11	6/11
Age (years)	26.5 (6.4) (range, 16–38)	26.5 (4.4) (range, 18–39)
Education (years)	14.7 (2.1)	15.1 (2.4)
Age of onset (years)	24.6 (6.6)	–
Duration of illness (years)	2.00 (2.1)	–
SAPS	35.5 (27.4)	–
SANS	52.6 (14.3)	–

Values represent mean (SD) SAPS; Scale for the Assessment of Positive Symptoms SANS; Scale for the Assessment of Negative Symptoms.

A recent development of imaging technique, such as LORETA and its modified versions (e.g. sLORETA), has improved the spatial resolution of EEG and event-related potentials by providing three-dimensional distribution pattern of these electrophysiological activities (Sumiyoshi et al., 2011). Using LORETA, Pascual-Marqui et al. (1999) reported asymmetrically enhanced delta band activities in the prefrontal cortex in neuroleptic-naïve, first-episode schizophrenia. On the other hand, Mientus et al. (2002) found an increase in delta band activity, most prominently in the anterior cingulate gyrus and temporal lobes, in unmedicated patients, while other frequency activities were not altered. These results suggest that enhanced delta band activity in the prefrontal cortex is associated with the pathophysiology of schizophrenia. However, there has been, to our knowledge, no study that addressed the correlation between delta band activity and the symptomatology of schizophrenia, e.g. positive and negative symptoms, using three-dimensional imaging methods, such as LORETA.

Negative symptoms of schizophrenia have been associated with structural impairment in the prefrontal cortex, and have been hypothesized to arise from decreased dopaminergic activity in this brain region (Lynch, 1992). Using SPECT, Molina Rodriguez et al. (1997) found severity of negative symptoms was negatively correlated with the degree of prefrontal lesions. Also, decreased glucose metabolism in the frontal cortex was associated with greater negative symptoms in subjects with schizophrenia (Potkin et al., 2002; Sabri et al., 1997). These previous observations indicate a role for prefrontal cortex in the psychopathology of schizophrenia, especially negative symptoms.

Taken together, it was hypothesized that aberrant neural activity in specific brain areas, as measured by electrophysiological methods, would be associated with psychotic symptoms, especially negative symptoms. In this study, we sought to determine (1) if some components of EEG, such as delta band activity, would be increased in brain areas relevant to the pathophysiology of schizophrenia, e.g. prefrontal cortex, and (2) if such electrical change would be associated with negative symptoms. To our knowledge, this study was the first to address these issues in neuroleptic-naïve patients using the LORETA imaging method.

2. Method

2.1. Subjects

Data were obtained from seventeen right-handed patients (female/male = 6/11) meeting DSM-IV-R criteria for schizophrenia (APA, 1994) at Toyama University Hospital. Demographic data for these patients are shown in Table 1. All patients were neuroleptic-naïve. Diagnosis was based on the Structured Clinical Interviews for DSM-IV (SCID). Psychiatric and treatment history was obtained from the patients, informants, and medical records. Subjects with current history of substance abuse or dependence, seizure, head injury and as any other medical condition known to interfere with EEG were excluded from the study. Eligible patients had a complete physical examination. Standard laboratory testing (blood count, liver and renal function, blood sugar, total cholesterol, and triglyceride) was normal. Clinical staff explained the nature of the study to the subjects, the risks and benefits, and the option not to participate in research. If the mental status of a subject was impaired to the point where s/he could not understand the nature of the study, its risks and benefits, or the option not to participate, the subjects was not approached to be in the research. This protocol was approved be the Committee on Medical Ethics of University of Toyama. After complete description of the study to the subjects, written informed consent was obtained. Fourteen patients were outpatients who were lightly and moderately ill without hospitalization. Three patients were in-patients. Seventeen age, gender, and education-matched right-handed healthy volunteers also participated in the study as control subjects. Demographic data for these control subjects are also shown in Table 1.

2.2. Design and procedure

The Scale for the Assessment of Positive Symptoms (SAPS; Andreasen, 1983b), and the Scales for the Assessment of Negative Symptoms (SANS; Andreasen, 1983a) were assessed by an experienced psychiatrist (Table 1).

Electroencephalograms (EEGs) were recorded with a 32-channel DC-amplifier (EEG-2100 version 2.22J, Nihon Kouden Corp., Tokyo, Japan). Recordings were performed using an electro-cap (Electro-cap Inc., Eaton, OH) in a sound-attenuated room. The EEG was recorded with 19 electrodes located at FP1, FP2, F3, F4, F7, F8, C3, C4, P3, P4, O1, O2, T3, T4, T5, T6, Fz, Cz, and Pz according to the international 10–20 system. All electrodes were referenced to the average amplitude of ear electrodes (bandwidth = 0.16–120 Hz, 60 Hz notch Filter). Electrode impedance was less than 10 kΩ. Data were controlled with a sampling rate of 256 Hz. Recording was conducted after eye closure for 5 min.

Off-line, the data were carefully screened for eye, muscle or eye-movement, and technical artifacts. Twenty 1-s epochs were available from all participants.

LORETA is a method to localize multiple distributed cortical sources of bioelectric activity in the three-dimensional space (Pascual-Marqui et al., 1994). In other words, LORETA demonstrates the synchronously activated neuronal populations underlying EEG activity by computing their cortical localization from the scalp distribution of the electric field. The LORETA inverse solution is based on existing neuroanatomical and physiological knowledge and a mathematical constraint called the smoothness assumption (Pascual-Marqui et al., 2002). The principles of LORETA and the mathematical tools have been described in details at http://www.uzh.ch/keyinst/NewLORETA/Software/Software.htm.

In order to mathematically mitigate the disturbing effects of the electrically conducting layers between the cortical surface and the electrodes, LORETA computes the inverse solution within a three-shell spherical head model including scalp, skull, and brain. The brain compartment of this model was restricted to the cortical grey matter and hippocampus, according to the Talairach Brain Atlas digitized at Montreal Neurological Institute (Talairach and Tournoux, 1988). The grey matter compartment was subdivided in 2394 voxels, which allows a spatial resolution of 7 mm. Cross-modal validation studies disclosed that LORETA and other functional neuroimaging methods showed the same cortical localization of dysfunction in several neuropsychiatric conditions (Pascual-Marqui et al., 2002).

We investigated the LORETA solution in seven frequency bands separately: Delta (1.5–6.0 Hz), theta (6.5–8.0 Hz), alpha-1 (8.5–10.0 Hz), alpha-2 (10.5–12.0 Hz), beta-1 (12.5–18.0 Hz), beta-2 (18.5–21.0 Hz), and beta-3 (21.5–30.0 Hz) were determined (Kubicki et al., 1979).

2.3. Statistical analyses

Group comparisons with respect to age and education were performed with the unpaired t test. The localization of the differences in activity between the groups was assessed by voxel-by-voxel nonpaired t test of the LORETA images, based on the power of estimated electric current density, which results in t statistic three dimensional images (Mientus et al., 2002). In these images, cortical voxels of statistically significant differences were identified by a nonparametric approach using randomization strategy that determined the critical probability threshold values for actually observed statistic with corrections for multiple testing (Holmes et al., 1996). Test results are presented as Figs. 1 and 2; and Table 2. Figures include information about the direction of changes between tested groups, either an increase (red-colored) or a decrease (blue-colored), and provide information about the significance of changes by indicating t-values that are significant at 0.1% level. LORETA specifications claim their corrected t for $P<0.05$ level as significant enough for testing 2394 voxels in one comparison (as used be other authors (Arai et al., 2003; Flor-Henry et al., 2004), however, a lower significance level (e.g. 5%) would have made it difficult to show the maximum areas of activation differences (Mientus et al., 2002). For all frequency bands, ROIs were chosen only for brain areas showing significant group-difference in LORETA values at 0.1% level.

Spearman's correlation coefficient was obtained to relate LORETA current density in these ROIs vs. SAPS and SANS scores. For this analysis, significance was set at 1% level for Bonferroni correction.

3. Results

Group comparisons between patients with schizophrenia and healthy control subjects revealed a significant increase in delta band activity for patients, with a maximum difference found at the left inferior temporal gyrus (ITG) (maximum $t=4.27$). A significant increase in delta band activities were also found for the right middle frontal gyrus (MFG) (maximum $t=4.26$), right inferior frontal gyrus (IFG) (maximum $t=4.16$), right superior frontal gyrus (SFG) (maximum $t=4.03$), and right parahippocampal gyrus (PHG) (maximum $t=4.03$) (Table 2, Fig. 1). Further, theta and alpha-2 frequency bands showed a trend-level increase (Table 2, Fig. 2). There were no significant group differences for alpha-1, beta-1, and beta-2 frequency bands.

Next, we determined correlations between the average of LORETA current density for delta band activity in the above 5 ROIs vs. SAPS and SANS Total scores. LORETA values for delta band activity at these brain regions (Table 3, Fig. 3) were negatively correlated with the SANS Total score. Specifically, the correlation for the ITG survived even after Bonferroni correction. On the other hand, there were no significant correlations between LORETA current density for delta band activity and the SAPS score.

4. Discussion

Patients with schizophrenia demonstrated an increase in LORETA values for delta band activity at several brain areas, including those in prefrontal cortex. Moreover, the increase in delta band activity was negatively associated with overall negative symptoms.

To our knowledge, our report is the first study which examined the correlations between specific band activity based on three-dimensional distribution of EEG and negative symptoms in neuroleptic-naïve patients with first-episode schizophrenia. LORETA current source images with 19 or more electrodes have been shown to provide good estimates of the localization for activated brain regions identified with f-MRI signals (Mulert et al., 2004; Sumiyoshi et al., 2009).

Koles et al. (2004) compared LORETA current densities from 57 male patients with schizophrenia and 65 matched control subjects. Comparisons were made during resting conditions and during verbal and spatial cognitive challenges. Results indicate that, for the delta band, significant differences in current density occupied the largest brain volume during the resting condition, with bilateral frontal regions showing increased current density. For the alpha band, the differences in current density occupied the smallest brain volume during the cognitive condition with decreased current density in schizophrenia in the right frontal region. In the beta band, the differences in current density occupied large brain volumes irrespective of cognitive state with increased current source density for schizophrenia. Data from all of the band frequencies in the resting condition, presented in the current study, confirm most of the previous findings with schizophrenia.

Increased delta activity in frontal regions in patients with schizophrenia is in agreement with other quantitative EEG (QEEG) and functional neuroimaging studies (Frith, 1997; Pascual-Marqui et al., 1999; Mientus et al., 2002; Tislerova et al., 2008). The increase in LORETA current density for delta band activity in the frontal and temporolimbic-occipital cortex in subjects with schizophrenia may provide an electrophysiological basis for aberrant function of frontal cortex (Ingvar et al., 1976; Guich et al., 1989), a notion supported by neuroimaging data (Ingvar and Franzen, 1974; Weinberger, 1987; Andreasen et al., 1992; Weinberger and Berman, 1996).

Tislerova et al. (2008) found an increase in the delta and theta frequencies over the fronto-temporo-occipital cortex, particularly in the temporolimbic structures, as well as an increase in alpha-1 and alpha-2 activities in the temporal cortex in neuroleptic-naïve patients with schizophrenia compared to healthy control subjects. They also found an increase in beta-1 and beta-2 in the temporo-occipital and posterior limbic structures in these patients. Mientus et al. (2002) reported an increase in delta activity, particularly in the anterior cingulate gyrus and left temporal lobes, in patients with unmedicated schizophrenia. These previous findings are generally in agreement with our observations (Table 2, Fig. 1).

The difference in delta band activity between patients and control subjects was largest at left ITG (Table 2, Fig. 1). Meisenzahl et al. (2008) reported that patients with first-episode schizophrenia revealed reduction in the volume of the left ITG compared to healthy controls. Also, grey matter volume reductions in the bilateral ITG have been reported in first episode (Kuroki et al., 2006) and chronic (Onitsuka et al., 2004) schizophrenia. Although there is little information about the role of ITG in the psychopathology of schizophrenia, our results reported here suggest the contribution of this brain area to affective disturbances of the illness.

The increase in delta band activity in the prefrontal cortex (MFG, IFG, and SFG), presented here, is consistent with the hypofrontality (Guich et al., 1989), which typically becomes apparent under a cognitive challenge. For example, patients with schizophrenia show deficits in working memory and executive function, as revealed, for example, by the Wisconsin Card Sorting Test (Buchsbaum et al., 1990; Andreasen et al., 1992; Tamminga et al., 1992; Hazlett et al., 2000; Ragland et al., 2007). An increase in delta band activity in the PHG and prefrontal cortex may be associated with a neural basis for cognitive deficits of schizophrenia. In this context, PHG has been shown to play an important role in verbal learning memory, a key domain of cognition relevant to social outcome (Sumiyoshi et al., 2006).

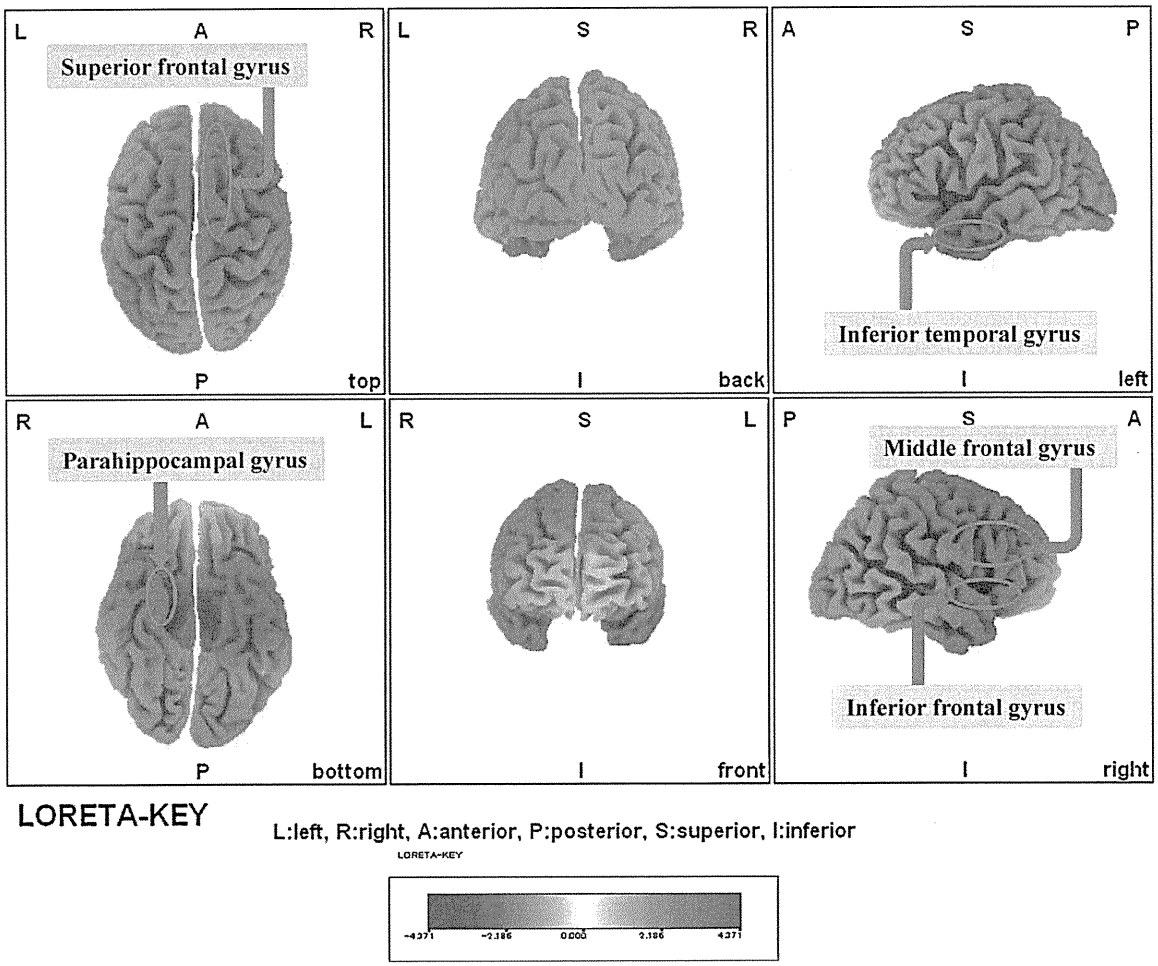

Fig. 1. Comparison of LORETA current density for delta band activity in patients with schizophrenia against normal control subjects as revealed by statistical non-parametric mapping (SnPM) voxel-wise LORETA comparisons for independent samples. Positive, zero, negative *t*-values are represented in red, white and blue, respectively. A significant increase ($P < 0.001$) in the LORETA current density for delta band activity for patients is shown in the left inferior temporal gyrus (ITG), right middle frontal gyrus (MFG), right superior frontal gyrus (SFG), right inferior frontal gyrus (IFG), and right parahippocampal gyrus (PHG).

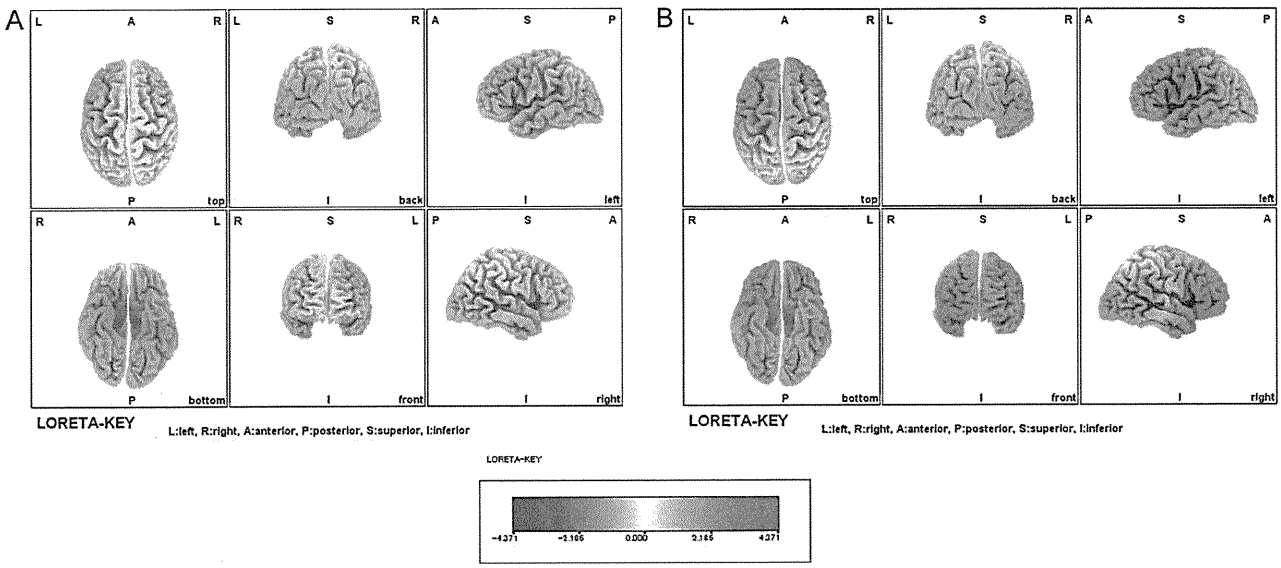

Fig. 2. Comparison of LORETA current density for theta (left) and alpha-2 (right) band activities in patients with schizophrenia against normal control subjects as revealed by statistical non-parametric mapping (SnPM) voxel-wise LORETA comparisons for independent samples. Positive, zero, negative *t*-values are represented in red, white and blue, respectively. A trend-level increase in the LORETA current density for theta (A) and alpha-2 (B) band activities is shown.

Table 2
Maximum difference of EEG activity in different frequency bands between patients with schizophrenia and healthy control subjects.

Frequency band	Extreme *t*-value	*P*-value	Extreme *t*-value: brain region predominantly involved		
			BA	Region	Right/Left
Delta (1.5–6.0 Hz)	4.37	<0.0001	20	Inferior temporal gyrus	L
Theta (6.5–8.5 Hz)	2.74	0.04	8	Middle frontal gyrus	R
Alpha-1 (8.5–10.0 Hz)	2.38	0.10	8	Superior frontal gyrus	R
Alpha-2 (10.5–12.0 Hz)	2.94	0.05	47	Inferior frontal gyrus	R
Beta-1 (12.5–18.0 Hz)	0.96	0.42	37	Parahippocampal gyrus	R
Beta-2 (18.5–21.0 Hz)	−1.75	0.19	34	Subcallosal gyrus	R
Beta-3 (21.5–30.0 Hz)	−2.06	0.06	47	Inferior temporal gyrus	R
			6	Precentral gyrus	L
			7	Precuneus	L
			7	Precuneus	L
			29	Posterior cingulate	L

Table 3
Spearman correlation coefficients between LORETA current density in discrete brain regions and SAPS and SANS Total score.

	SAPS		SANS	
	r	*P*	*r*	*P*
Right superior frontal gyrus	−0.20	n.s.	−0.54	0.02
Right middle frontal gyrus	−0.31	n.s.	−0.56	0.02
Right inferior frontal gyrus	−0.13	n.s.	−0.52	0.03
Right parahippocampal gyrus	−0.05	n.s.	−0.50	0.04
Left inferior temporal gyrus	−0.19	n.s.	−0.60	0.01

Another important finding in this study was that LORETA current density of delta activity in the left ITG was negatively correlated with severity of negative symptoms. Coutin-Churchman and Moreno (2008) reported that alcoholic patients with depressive symptoms showed significantly lower current density of delta band activity in the left temporal cortical areas, as well as medial temporal areas, including amygdala and hippocampus, compared to non-depressed patients. On the other hand, right frontopolar cortex and superior temporal cortex of depressed subjects showed increased delta activity. They also found that current densities in delta band activity at left parahippocampal cortex, left midfrontal cortex and right frontopolar cortex were negatively correlated with the Beck Depression Inventory (BDI) score. A negative correlation between delta power in the frontal areas and the BDI score was also reported in a magnetoencephalographic study (Wienbruch et al., 2003). These latter findings are in line with the results reported here (Table 2), showing an association between enhanced delta band activity and severity of negative symptoms, including affective disturbances.

Tislerova et al. (2008) reported that clozapine enhances LORETA current source density for delta and theta bands activity in the anterior cingulate cortex and medial frontal cortex in neuroleptic-naïve patients with schizophrenia. Another study (Gross et al., 2004) reports that the greater improvement in negative symptoms by treatment with clozapine was associated with the larger increase in 3.5–7.0 Hz power band activity in fronto-central areas. Together with the link between the increased delta band activity in prefrontal cortex and fewer negative symptoms (Table 2), the results of these previous studies suggest that an increase in slow activity in specific brain regions may represent a compensatory mechanism against the pathological process intrinsic to schizophrenia.

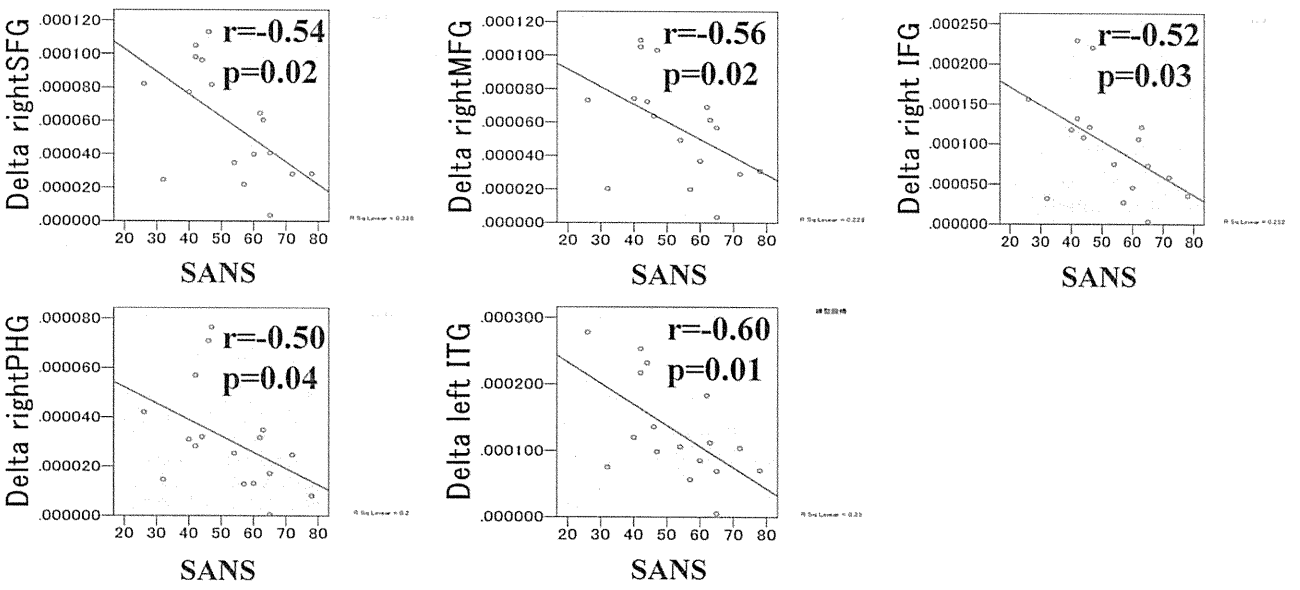

Fig. 3. Correlations between LORETA current density and SANS Total score for respective ROIs in subjects with schizophrenia (see Section 3).

Dang-Vu et al. (2008) found transient changes in brain activity to be consistently associated with slow wave (>140 μV) and delta wave (75–140 μV) during slow wave sleep (SWS) in 14 healthy control subjects. Significant increases in activity were related to these waves in several cortical areas, including the inferior temporal, medial prefrontal, precuneus, and posterior cingulate areas. Compared with baseline activity, slow waves were associated with significant activity in the parahippocampal gyrus, cerebellum, and brainstem, whereas delta waves were related to frontal responses (Dang-Vu et al., 2008). They concluded that SWS is not a state of brain quiescence, but rather is an active state during which brain activity is consistently synchronized to the slow oscillation in specific cerebral regions (Dang-Vu et al., 2008). Their results are in line with our contention that slow waves, such as delta band activity, may be an "active condition" which is likely to compensate for the pathological conditions in schizophrenia.

Harmony et al. (1996) argued that an increase in delta EEG activity during mental tasks may be related to subjects' attention to internal processing. Therefore, an increase of delta band activity might be related to a mechanism of reducing external input, that is, subjects who are capable of reducing inputs might also be able to cope better with psychosis, and have less secondary negative symptoms. We also found a trend-level increase in theta and alpha-2 band activities in patients with schizophrenia. Previous QEEG studies report an increase in theta activity in subjects with schizophrenia. For example, Veiga et al. (2003) observed that patients with chronic schizophrenia show increased delta and theta frequency bands activity in brain areas, such as the right middle frontal gyrus, right inferior temporal gyrus, and right insula, as well as bilateral anterior cingulate gyrus, using LORETA. These previous data from chronic patients and the present results from first-episode patients indicate that increased slow activity in frontal regions is independent of the clinical stage, and thus, intrinsic to schizophrenia.

Some studies report an increase in the alpha power over the frontal regions in schizophrenia (Nakagawa et al., 1991; Kahn et al., 1993). A recent analysis of the current density distribution also showed "anteriorization" of alpha activity in first-episode schizophrenia (Begre et al., 2003), which is in partial agreement with the current data showing a trend-level increase in alpha-2 band activity in the patients (Table 2, Fig. 2).

A major limitation in our study is the relatively small number of subjects. This might have confounded some of the present results, e.g. correlations between delta band activities vs. negative symptoms.

5. Conclusion

In conclusion, LORETA analysis of three-dimensional distribution of EEG current density suggest aberrant electrophysiological activity in some brain regions, e.g. prefrontal cortex, is associated with negative symptoms. Increased delta band activity, related to fewer negative symptoms, may represent a response to the pathological process intrinsic to schizophrenia.

Acknowledgements

This work was supported by Health and Labour Sciences Research Grants from the Ministry of Health, Labour, and Welfare, and by grants-in-aid for Scientific Research from the Japan Society for the Promotion of Science to Tomiki Sumiyoshi.

References

American Psychiatric Assocatation, 1994. Diagnostic and Statistical Manual of Mental Disorders, 4th ed. (DSM-IV). APA. Washington D.C.

Andreasen, N.C., 1983a. Scale for the Assessment of Negative Symptoms (SANS). University of Iowa, Iowa City.

Andreasen, N.C., 1983b. Scale for the Assessment of Positive Symptoms (SAPS). University of Iowa, Iowa City.

Andreasen, N.C., Rezai, K., Alliger, R., Swayze 2nd, V.W., Flaum, M., Kirchner, P., Cohen, G., O'Leary, D.S., 1992. Hypofrontality in neuroleptic-naive patients and in patients with chronic schizophrenia. Assessment with xenon 133 single-photon emission computed tomography and the Tower of London. Arch. Gen. Psychiatr. 49, 943–958.

Andreasen, N.C., O'Leary, D.S., Flaum, M., Nopoulos, P., Watkins, G.L., Boles Ponto, L.L., Hichwa, R.D., 1997. Hypofrontality in schizophrenia: distributed dysfunctional circuits in neuroleptic-naive patients. Lancet 349, 1730–1734.

Arai, M., Tanaka, H., Pascual-Marqui, R.D., Hirata, K., 2003. Reduced brain electric activities of frontal lobe in cortical cerebellar atrophy. Clin. Neurophysiol. 114, 740–747.

Begre, S., Federspiel, A., Kiefer, C., Schroth, G., Dierks, T., Strik, W.K., 2003. Reduced hippocampal anisotropy related to anteriorization of alpha EEG in schizophrenia. Neuroreport 14, 739–742.

Buchsbaum, M.S., Nuechterlein, K.H., Haier, R.J., Wu, J., Sicotte, N., Hazlett, E., Asarnow, R., Potkin, S., Guich, S., 1990. Glucose metabolic rate in normals and schizophrenics during the Continuous Performance Test assessed by positron emission tomography. Br. J. Psychiatr. 156, 216–227.

Cleghorn, J.M., Garnett, E.S., Nahmias, C., Firnau, G., Brown, G.M., Kaplan, R., Szechtman, H., Szechtman, B., 1989. Increased frontal and reduced parietal glucose metabolism in acute untreated schizophrenia. Psychiatr. Res. 28, 119–133.

Coutin-Churchman, P., Moreno, R., 2008. Intracranial current density (LORETA) differences in QEEG frequency bands between depressed and non-depressed alcoholic patients. Clin. Neurophysiol. 119, 948–958.

Crow, T.J., 1980. Molecular pathology of schizophrenia: more than one disease process? Br. Med. J. 280, 66–68.

Dang-Vu, T.T., Schabus, M., Desseilles, M., Albouy, G., Boly, M., Darsaud, A., Gais, S., Rauchs, G., Sterpenich, V., Vandewalle, G., Carrier, J., Moonen, G., Balteau, E., Degueldre, C., Luxen, A., Phillips, C., Maquet, P., 2008. Spontaneous neural activity during human slow wave sleep. Proc. Natl. Acad. Sci. U. S. A. 105, 15160–15165.

Flor-Henry, P., Lind, J.C., Koles, Z.J., 2004. A source-imaging (low-resolution electromagnetic tomography) study of the EEGs from unmedicated males with depression. Psychiatr. Res. 130, 191–207.

Frith, C.D., 1997. Functional brain imaging and the neuropathology of schizophrenia. Schizophr. Bull. 23, 525–527.

Gross, A., Joutsiniemi, S.L., Rimon, R., Appelberg, B., 2004. Clozapine-induced QEEG changes correlate with clinical response in schizophrenic patients: a prospective, longitudinal study. Pharmacopsychiatry 37, 119–122.

Guich, S.M., Buchsbaum, M.S., Burgwald, L., Wu, J., Haier, R., Asarnow, R., Nuechterlein, K., Potkin, S., 1989. Effect of attention on frontal distribution of delta activity and cerebral metabolic rate in schizophrenia. Schizophr. Res. 2, 439–448.

Harmony, T., Fernández, T., Silva, J., Bernal, J., Díaz-Comas, L., Reyes, A., Marosi, E., Rodríguez, M., Rodríguez, M., 1996. EEG delta activity: an indicator of attention to internal processing during performance of mental tasks. Int. J. Psychophysiol. 24 (1–2), 161–171.

Hazlett, E.A., Buchsbaum, M.S., Jeu, L.A., Nenadic, I., Fleischman, M.B., Shihabuddin, L., Haznedar, M.M., Harvey, P.D., 2000. Hypofrontality in unmedicated schizophrenia patients studied with PET during performance of a serial verbal learning task. Schizophr. Res. 43, 33–46.

Holmes, A.P., Blair, R.C., Watson, J.D., Ford, I., 1996. Nonparametric analysis of statistic images from functional mapping experiments. J. Cereb. Blood Flow Metab. 16, 7–22.

Ingvar, D.H., Franzen, G., 1974. Abnormalities of cerebral blood flow distribution in patients with chronic schizophrenia. Acta Psychiatr. Scand. 50, 425–462.

Ingvar, D.H., Sjolund, B., Ardo, A., 1976. Correlation between dominant EEG frequency, cerebral oxygen uptake and blood flow. Electroencephalogr. Clin. Neurophysiol. 41, 268–276.

Kahn, E.M., Weiner, R.D., Coppola, R., Kudler, H.S., Schultz, K., 1993. Spectral and topographic analysis of EEG in schizophrenic patients. Biol. Psychiatr. 33, 284–290.

Koles, Z.J., Lind, J.C., Flor-Henry, P., 2004. A source-imaging (low-resolution electromagnetic tomography) study of the EEGs from unmedicated men with schizophrenia. Psychiatry Res. 130, 171–190.

Kubicki, S., Herrmann, W.M., Fichte, K., Freund, G., 1979. Reflections on the topics: EEG frequency bands and regulation of vigilance. Pharmakopsychiatr. Neuropsychopharmakol. 12, 237–245.

Kuroki, N., Shenton, M.E., Salisbury, D.F., Hirayasu, Y., Onitsuka, T., Ersner-Hershfield, H., Yurgelun-Todd, D., Kikinis, R., Jolesz, F.A., McCarley, R.W., 2006. Middle and inferior temporal gyrus gray matter volume abnormalities in first-episode schizophrenia: an MRI study. Am. J. Psychiatr. 163, 2103–2110.

Lynch, M.R., 1992. Schizophrenia and the D1 receptor: focus on negative symptoms. Prog. Neuropsychopharmacol. Biol. Psychiatr. 16, 797–832.

Meisenzahl, E.M., Koutsouleris, N., Bottlender, R., Scheuerecker, J., Jager, M., Teipel, S.J., Holzinger, S., Frodl, T., Preuss, U., Schmitt, G., Burgermeister, B., Reiser, M., Born, C., Moller, H.J., 2008. Structural brain alterations at different stages of schizophrenia: a voxel-based morphometric study. Schizophr. Res. 104, 44–60.

Mientus, S., Gallinat, J., Wuebben, Y., Pascual-Marqui, R.D., Mulert, C., Frick, K., Dorn, H., Herrmann, W.M., Winterer, G., 2002. Cortical hypoactivation during resting EEG in schizophrenics but not in depressives and schizotypal subjects as revealed by low resolution electromagnetic tomography (LORETA). Psychiatr. Res. 116, 95–111.

Molina Rodriguez, V., Montz Andree, R., Perez Castejon, M.J., Gutierrez Labrador, R., Ferre Navarrete, F., Carreas Delgado, J.L., Rubia Vila, F.J., 1997. Cerebral perfusion correlates of negative symptomatology and Parkinsonism in a sample of treatment-refractory schizophrenics: an exploratory 99mTc-HMPAO SPET study. Schizophr. Res. 25, 11–20.

Mulert, C., Jager, L., Schmitt, R., Bussfeld, P., Pogarell, O., Moller, H.J., Juckel, G., Hegerl, U., 2004. Integration of fMRI and simultaneous EEG: towards a comprehensive understanding of localization and time-course of brain activity in target detection. Neuroimage 22, 83–94.

Nakagawa, M., Takeda, K., Kakimoto, Y., 1991. Characteristic distribution of alpha 2 wave in electroencephalograms of schizophrenic patients during discriminative tasks: support for the hypofrontality hypothesis of schizophrenia. Acta Psychiatr. Scand. 83, 105–114.

Onitsuka, T., Shenton, M.E., Salisbury, D.F., Dickey, C.C., Kasai, K., Toner, S.K., Frumin, M., Kikinis, R., Jolesz, F.A., McCarley, R.W., 2004. Middle and inferior temporal gyrus gray matter volume abnormalities in chronic schizophrenia: an MRI study. Am. J. Psychiatr. 161, 1603–1611.

Parellada, E., Catafau, A.M., Bernardo, M., Lomena, F., Gonzalez-Monclus, E., Setoain, J., 1994. Prefrontal dysfunction in young acute neuroleptic-naive schizophrenic patients: a resting and activation SPECT study. Psychiatr. Res. 55, 131–139.

Pascual-Marqui, R.D., Michel, C.M., Lehmann, D., 1994. Low resolution electromagnetic tomography: a new method for localizing electrical activity in the brain. Int. J. Psychophysiol. 18, 49–65.

Pascual-Marqui, R.D., 1995. Continuing discussion of the inverse problem. ISBET Newsletter (ISSN 0947-5133), pp. 9–30.

Pascual-Marqui, R.D., Lehmann, D., Koenig, T., Kochi, K., Merlo, M.C., Hell, D., Koukkou, M., 1999. Low resolution brain electromagnetic tomography (LORETA) functional imaging in acute, neuroleptic-naive, first-episode, productive schizophrenia. Psychiatr. Res. 90, 169–179.

Pascual-Marqui, R.D., Esslen, M., Kochi, K., Lehmann, D., 2002. Functional imaging with low-resolution brain electromagnetic tomography (LORETA): a review. Method Find. Exp. Clin. Pharmacol. 24 (Suppl. C), 91–95.

Pizzagalli, D., Pascual-Marqui, R.D., Nitschke, J.B., Oakes, T.R., Larson, C.L., Abercrombie, H.C., Schaefer, S.M., Koger, J.V., Benca, R.M., Davidson, R.J., 2001. Anterior cingulate activity as a predictor of degree of treatment response in major depression: evidence from brain electrical tomography analysis. Am. J. Psychiatr. 158, 405–415.

Potkin, S.G., Alva, G., Fleming, K., Anand, R., Keator, D., Carreon, D., Doo, M., Jin, Y., Wu, J.C., Fallon, J.H., 2002. A PET study of the pathophysiology of negative symptoms in schizophrenia Positron emission tomography. Am. J. Psychiatr. 159, 227–237.

Ragland, J.D., Yoon, J., Minzenberg, M.J., Carter, C.S., 2007. Neuroimaging of cognitive disability in schizophrenia: search for a pathophysiological mechanism. Int. Rev. Psychiatr. 19, 417–427.

Sabri, O., Erkwoh, R., Schreckenberger, M., Owega, A., Sass, H., Buell, U., 1997. Correlation of positive symptoms exclusively to hyperperfusion or hypoperfusion of cerebral cortex in never-treated schizophrenics. Lancet 349, 1735–1739.

Sumiyoshi, T., Higuchi, Y., Itoh, T., Matsui, M., Arai, H., Suzuki, M., Kurachi, M., Sumiyoshi, C., Kawasaki, Y., 2009. Effect of perospirone on P300 electrophysiological activity and social cognition in schizophrenia: A three-dimensional analysis with sLORETA. Psychiatr. Res. Neuroimaging. 172, 180–183.

Sumiyoshi, T., Higuchi, Y., Itoh, T., Kawasaki, Y., 2011. Electrophysiological imaging evaluation of schizophrenia and treatment response. Handbook of Schizophrenia Spectrum Disorders, vol. 3, Nova Science Publishers, New York.(in press).

Sumiyoshi, T., Matsui, M., Yamashita, I., Nohara, S., Uehara, T., Kurachi, M., Meltzer, H.Y., 2000. Effect of adjunctive treatment with serotonin-1A agonist tandospirone on memory functions in schizophrenia. J. Clin. Psychopharmacol. 20, 386–388.

Sumiyoshi, T., Sumiyoshi, C., Nohara, S., Hagino, H., Hasegawa, S., Kuwayama, N., Endo, S., Kurachi, M., 2006. Verbal memory deficits in a preadolescent case of lesions of the left parahippocampal gyrus associated with a benign tumor. Prog. Neuropsychopharmacol. Biol. Psychiatr. 30, 733–736.

Talairach, J., Tournoux, P., 1988. Co-planar Stereotaxic Atlas of the Human Brain: Three-Dimensional Proportional System. G. Thieme, Stuttgart.

Tamminga, C.A., Thaker, G.K., Buchanan, R., Kirkpatrick, B., Alphs, L.D., Chase, T.N., Carpenter, W.T., 1992. Limbic system abnormalities identified in schizophrenia using positron emission tomography with fluorodeoxyglucose and neocortical alterations with deficit syndrome. Arch. Gen. Psychiatr. 49, 522–530.

Tislerova, B., Brunovsky, M., Horacek, J., Novak, T., Kopecek, M., Mohr, P., Krajca, V., 2008. LORETA functional imaging in antipsychotic-naive and olanzapine-, clozapine- and risperidone-treated patients with schizophrenia. Neuropsychobiology 58, 1–10.

Veiga, H., Deslandes, A., Cagy, M., Fiszman, A., Piedade, R.A., Ribeiro, P., 2003. Neurocortical electrical activity tomography in chronic schizophrenics. Arq. Neuropsiquiatr. 61, 712–717.

Weinberger, D.R., 1987. Implications of normal brain development for the pathogenesis of schizophrenia. Arch. Gen. Psychiatr. 44, 660–669.

Weinberger, D.R., Berman, K.F., 1996. Prefrontal function in schizophrenia: confounds and controversies. Philos. Trans. R. Soc. Lond. B: Biol. Sci. 351, 1495–1503.

Wienbruch, C., Moratti, S., Elbert, T., Vogel, U., Fehr, T., Kissler, J., Schiller, A., Rockstroh, B., 2003. Source distribution of neuromagnetic slow wave activity in schizophrenic and depressive patients. Clin. Neurophysiol. 114, 2052–2060.

Clinical Neurophysiology 122 (2011) 1533–1540

Contents lists available at ScienceDirect

Clinical Neurophysiology

journal homepage: www.elsevier.com/locate/clinph

Association between severe dorsolateral prefrontal dysfunction during random number generation and earlier onset in schizophrenia

Shinsuke Koike *, Ryu Takizawa, Yukika Nishimura, Kohei Marumo, Masaru Kinou, Yuki Kawakubo, Mark A. Rogers, Kiyoto Kasai

Department of Neuropsychiatry, Graduate School of Medicine, The University of Tokyo, Tokyo, Japan

ARTICLE INFO

Article history:
Accepted 23 December 2010
Available online 16 February 2011

Keywords:
Schizophrenia
Age at onset
Random number generation (RNG)
Short-term memory
Near-infrared spectroscopy (NIRS)
Prefrontal cortical haemodynamics

HIGHLIGHTS

- This study addresses the need for an objective assessment tool evaluating prefrontal function and social outcome non-invasively in the clinical setting.
- Such a tool would be valuable for studies of the pathophysiology of schizophrenia and in the evaluation of patients with schizophrenia.
- Multichannel near-infrared spectroscopy is a non-invasive and user-friendly instrument, and may be useful in evaluating cognitive function and social outcome in clinical settings in psychiatry.

ABSTRACT

Objectives: Schizophrenia involves impairment in attention, working memory and executive processes associated with prefrontal cortical function, an essential contributor of social functioning. Age at onset is a major factor for predicting social outcome in schizophrenia. In clinical settings, we need an objective assessment tool for evaluating prefrontal function and social outcome.
Methods: Participants included 22 right-handed patients with schizophrenia and 40 gender- and age-matched healthy controls. We used a 52-channel near-infrared spectroscopy (NIRS) instrument to measure oxygenated haemoglobin ([oxy-Hb]) changes over the prefrontal cortex during a random number generation (RNG) task.
Results: In healthy controls, we found significant [oxy-Hb] increase in the bilateral dorsolateral (DLPFC; BA9 and BA46) and ventrolateral prefrontal cortex (VLPFC; BA44, 45 and 47). The patients with schizophrenia showed significantly smaller activation than the healthy controls in the same approximate regions. In the patient group, a smaller [oxy-Hb] increase in the right DLPFC region (BA9) was significantly correlated with earlier age at onset.
Conclusions: NIRS can detect prefrontal cortical dysfunction associated with an executive task, which was coupled with earlier age at onset in schizophrenia.
Significance: Multichannel NIRS, a non-invasive and user-friendly instrument, may be useful in evaluating cognitive function and social outcome in clinical settings in psychiatry.

1. Introduction

Age at onset of schizophrenia is assumed to be one of the major risk factors that worsen symptoms and cognitions, and consequently influences occupational and social deficits (Eggers and Bunk, 1997; Hafner, 2000). In recent years, therefore, some research groups have tried to delay and finally prevent the onset of schizophrenia in adolescents (Brewer et al., 2005; Hafner, 2000; McGlashan et al., 2006; McGorry et al., 2002). However, it has been difficult to predict the onset of schizophrenia with clinical assessment, and neuropsychological or neuroimaging tools that could be easily applied in a practical clinical setting have never been developed.

The random number generation (RNG) task is one of neuropsychological tasks used to assess functional abnormalities in the frontotemporal cortex, which requires participants to generate random digits at equal intervals. The RNG task requires the ability not only to inhibit competing or habitual responses, but also requires attention, working memory and executive processes, all of

* Corresponding author. Address: Department of Neuropsychiatry, Graduate School of Medicine, The University of Tokyo, 7-3-1 Hongo, Bunkyo-ku, Tokyo 113-8655, Japan. Tel.: +81 3 5800 9263; fax: +81 3 5800 6894.
E-mail address: skoike-tky@umin.ac.jp (S. Koike).

1388-2457/$36.00 © 2011 International Federation of Clinical Neurophysiology. Published by Elsevier Ireland Ltd. All rights reserved.
doi:10.1016/j.clinph.2010.12.056

which are related to prefrontal cortical functions (Baddeley and Wilson, 1988; Ginsburg and Karpiuk, 1994). The RNG task requires less specificity for a certain function than other neurocognitive tasks, such as n-back task for working memory, but rather requires coordinating these functions related in a major way to the prefrontal cortex (PFC). Furthermore, the RNG task can measure prefrontal dysfunction easily in clinical settings. Patients with schizophrenia showed lower performance than controls (Hoshi et al., 2006; Peters et al., 2007; Shinba et al., 2004), but showed performance similar to patients with other frontal dysfunctions, such as Alzheimer's disease (Brugger et al., 1996), and frontal injuries (Spatt and Goldenberg, 1993).

A functional neuroimaging study using positron emission tomography (PET) showed that healthy participants had increased activation in the right inferior frontal cortex, the left dorsolateral prefrontal cortex (DLPFC) and the bilateral cerebellum during the RNG task (Jahanshahi et al., 2000). A functional magnetic resonance imaging (fMRI) study also showed that healthy participants had increased activation bilaterally in the DLPFC, the lateral premotor cortex, the anterior cingulate, the inferior and superior parietal cortex and in the cerebellar hemispheres (Daniels et al., 2003).

A near-infrared spectroscopy (NIRS) technique can measure the signals that reflect haemodynamic oxygenated haemoglobin ([oxy-Hb]) and deoxygenated haemoglobin ([deoxy-Hb]) changes in the cerebral cortex, while functional brain imaging methodologies such as fMRI and PET instruments are limited because of their large apparatuses, which prevent their use at a bedside setting for diagnostic and treatment purposes. The advantages of NIRS are its non-invasiveness, easy set-up, minimal constraint, rather small machinery and quietness. In addition, NIRS instruments with multichannels can evaluate the spatio-temporal characteristics of cortical function, and have considerable replicability of signal changes over the PFC in repetitive measurements (Kakimoto et al., 2009; Kono et al., 2007). Accordingly, NIRS has been used to assess brain functions in many psychiatric disorders, including schizophrenia (Fallgatter and Strik, 2000; Hoshi et al., 2006; Lee et al., 2008; Shinba et al., 2004; Suto et al., 2004; Takizawa et al., 2008, 2009), bipolar disorder (Matsuo et al., 2007), depression (Matsuo et al., 2005), post-traumatic stress disorder (Matsuo et al., 2003), panic disorder (Nishimura et al., 2007) and pervasive developmental disorders (Kuwabara et al., 2006). Even though it has also been indicated that patients with schizophrenia had reduced activation in the PFC using a two-channel NIRS instrument during the RNG task (Hoshi et al., 2006; Shinba et al., 2004), these studies had difficulty in detecting differential spatio-temporal characteristics. Our multichannel NIRS study showed reduced activations of the frontopolar region, rather than other prefrontal regions, and showed significant positive correlations with lower global assessment of functioning (GAF) scores in the schizophrenia group (Takizawa et al., 2008). Therefore, multichannel NIRS instruments could be useful in evaluating the spatio-temporal activation patterns in the prefrontal sub-regions.

In this study, we measured the change in prefrontal activation during the RNG task in patients with schizophrenia and healthy controls by using a 52 multichannel NIRS instrument with a wide coverage over the prefrontal cortical surface area. Furthermore, we sought to explore the relationship between haemodynamic prefrontal responses and age at onset in patients with schizophrenia.

2. Methods

2.1. Participants

Participants included 22 patients with schizophrenia and 40 gender- and age-matched healthy controls. All participants were right handed (>70 in the Edinburgh handedness scale (Oldfield, 1971)). They gave written informed consent to the ethical committee of the Faculty of Medicine, University of Tokyo (approval number 630-5), according to the Declaration of Helsinki, after a complete explanation of this study. The patients with schizophrenia were recruited among outpatients and inpatients at the University of Tokyo Hospital. One experienced psychiatrist, K.K., diagnosed with the Structured Clinical Interview for DSM-IV Axis I Disorders (First et al., 2003). The exclusion criteria for both groups were neurological illness, traumatic brain injury with any known cognitive consequences or loss of consciousness for more than 5 min, a history of electroconvulsive therapy, low premorbid Intelligence Quotient (IQ) (below 70) and previous alcohol/substance abuse or addiction. The exclusion criterion for the control group was a previous psychiatric disorder in themselves or a family history of psychotic disorders in their first-degree relatives. To rule out psychiatric disorders in healthy controls, we used the modified Mini-International Neuropsychiatric Interview for all control participants (Otsubo et al., 2005).

On the same day as the NIRS measurement, all participants were assessed using the GAF (American Psychiatric Association, 1994) and the socioeconomic status (SES) and parental SES using the Hollingshead scale (Hollingshead, 1965) (Table 1). In the patients with schizophrenia, we evaluated their psychiatric symptoms by using the Positive and Negative Syndrome Scale (PANSS) (Kay et al., 1987). To verify the age at onset of schizophrenia, we interviewed the patients and one of their family members in detail to obtain a history of their symptoms around their initial psychotic periods, and retrospectively estimated the age at onset in accordance with Addington et al. (2004). The onset of schizophrenia is defined by the presence of first positive symptoms (hallucinations, delusions or thought disorder) rated as above 4 on the PANSS and lasting throughout the day for several days or several times a week, not being limited to a few brief moments (Addington et al., 2004). At the time of the experiment, all patients received antipsychotics and/or anxiolytics and/or antiparkinsonian agents; therefore, we assessed their dose of medication and calculated equivalent doses of chlorpromazine, diazepam and biperiden, respectively (American Psychiatric Association, 1997).

Table 1
Demographic characteristics and performance of random number generation task in patients with schizophrenia (SZ) and healthy controls (HC).

	HC (n = 40)		SZ (n = 22)		p-Value
	Mean	SD	Mean	SD	
Male	20	N.A.	11	N.A.	1.0
Age (years)	36.8	15.3	41.0	11.6	0.238
Education (year)	15.3	1.6	14.5	2.8	0.200
Participant's SES[a]	2.0	0.6	3.6	1.1	<0.001
PANSS scores[b]					
Positive	N.A.	N.A.	16.3	4.2	N.A.
Negative	N.A.	N.A.	23.0	6.3	N.A.
General	N.A.	N.A.	38.8	7.6	N.A.
GAF[c]	N.A.	N.A.	46.7	11.9	N.A.
Age at onset (years)	N.A.	N.A.	26.3	8.8	N.A.
DUP (weeks)[d]	N.A.	N.A.	44.5	49.2	N.A.
DOI (years)[e]	N.A.	N.A.	14.7	8.8	N.A.
Chlorpromazine eq. (mg)	N.A.	N.A.	809	674	N.A.
Diazepam eq. (mg)	N.A.	N.A.	10.5	13.1	N.A.
Biperiden eq. (mg)	N.A.	N.A.	4.1	2.1	N.A.
RNG index	0.112	0.034	0.194	0.184	0.0497

N.A., not applicable.
[a] SES, socioeconomic status.
[b] PANSS, Positive and Negative Syndrome Scale.
[c] GAF, the global assessment of functioning.
[d] DUP, duration of untreated psychosis.
[e] DOI, duration of illness.

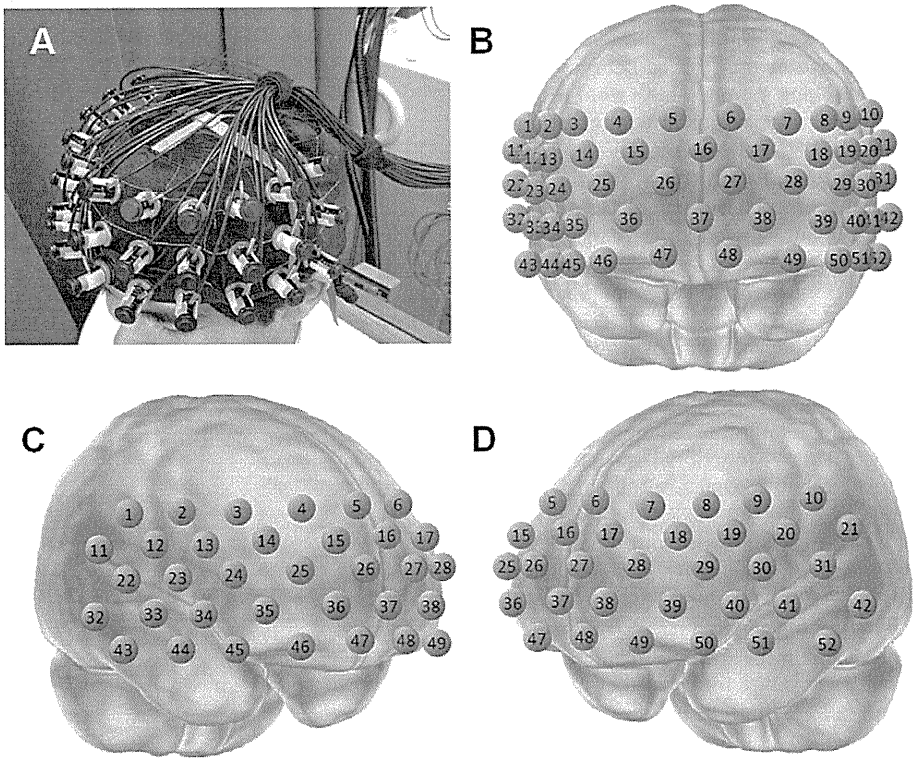

Fig. 1. The probe setting and measurement points of 52-channel near-infrared spectroscopy (NIRS). (A) The probes with thermoplastic 3 × 11 shells were placed over a subject's bilateral frontal regions. (B–D) The 52 measuring positions of the NIRS machine are superimposed on a 3D-reconstructed cerebral cortical surface from the Montreal Neurological Institute (MNI) Colin27 average MRI image (B, frontal view; C, right anterior oblique view; D, left anterior oblique view). The channel numbers are indicated above the measuring points.

2.2. RNG task

We divided the RNG task into three periods; counting, activation and post-activation periods. During the 60-s activation period, we instructed the participants to generate and call out random digits from 1 to 9 by using 1-Hz pacing, and noted their generated numbers correctly. During the 30-s counting and 70-s post-activation periods, they were asked to repeat aloud a sequence of digits from 1 to 9, guided by 1-Hz pacing. The pacing rate (every 1 s) was controlled with a metronome sound throughout the task. All participants performed a short training version of this task at least twice and then performed the RNG task. In this study, we defined 'valid response' as saying a correct digit aloud along with the metronome sound, and adopted those participants who could achieve a greater than 90% valid response during the activation period.

We calculated the RNG index for analysing their performance in generating random numbers (Evans, 1978) because the RNG index has a high test–retest stability and has been preferentially used in previous studies in schizophrenia. The RNG index measures the difference between expected and observed probabilities of pairs of consecutive digits. For example, if a participant selects more specific patterns (mostly '3' following '7'), the number of pairs of consecutive digits (the pair '37') increases so that the difference between ideal and actual frequencies of the pairs becomes wider. Ideal randomness is measured as 0 and pure non-randomness would be 1 in the RNG index (Evans, 1978).

2.3. NIRS measurement

We used a 52-channel NIRS instrument (ETG-4000, Hitachi Medical Co.). The participants only needed to sit in a chair in a relaxed state with their eyes open, and cap the thermoplastic attachment of the NIRS probes on their head. To minimise motion artefacts, we instructed them to avoid physical motions, such as head movement and strong biting, during the measurement. The NIRS probe attachment was a thermoplastic 3 * 11 shell and set with 52 fixed channels (Fig. 1). The lowest probe line was set along the Fp1–Fp2 line defined by the international 10–20 system used in electroencephalography. The 52 measuring areas are labelled ch1–ch52 from the right posterior to the left anterior. This arrangement of probes can measure [Hb] from the bilateral prefrontal (approximately dorsolateral (Brodmann's area (BA) 9, 46), ventrolateral (BA 44, 45 and 47), and frontopolar (BA 10)) and superior temporal cortical surface regions (Fig. 1).

The theoretical methodology of haemoglobin concentration measurement using NIRS instruments has been described in details elsewhere (Takizawa et al., 2008), but is briefly described as follows. The NIRS instrument measures relative changes in [oxy-Hb] and [deoxy-Hb] using two wavelengths (695 and 830 nm) of infrared light, based on the Beer–Lambert law (Watanabe et al., 1996; Yamashita et al., 1996). In this continuous-wave NIRS system, the [Hb] values include a differential path-length factor (DPF). The distance between pairs of source-detector probes was set at 3.0 cm, and we defined each measurement area between pairs of source-detector probes as one 'channel'. It is assumed that an NIRS system, in which the source-detector spacing is 3.0 cm, measures points at a 2–3 cm depth from the scalp, that is, the surface of the cerebral cortex (Okada and Delpy, 2003).

We set the time resolution of NIRS signals at 0.1 s. Because the NIRS signal was sometimes unstable at the start of the measurement due to technical issues and/or some effects of participant's tense state and thoughts before starting the task, the pre-task baseline was determined as the mean across the last 10 s of the pre-task period and the post-task baseline was determined as the mean across the last 5 s of the post-task period, and a linear fitting was performed on the basis of the data between the two baselines (Fig. 2). Moving average methods were applied to remove short-term motion artefacts in the analysed data (moving average win-

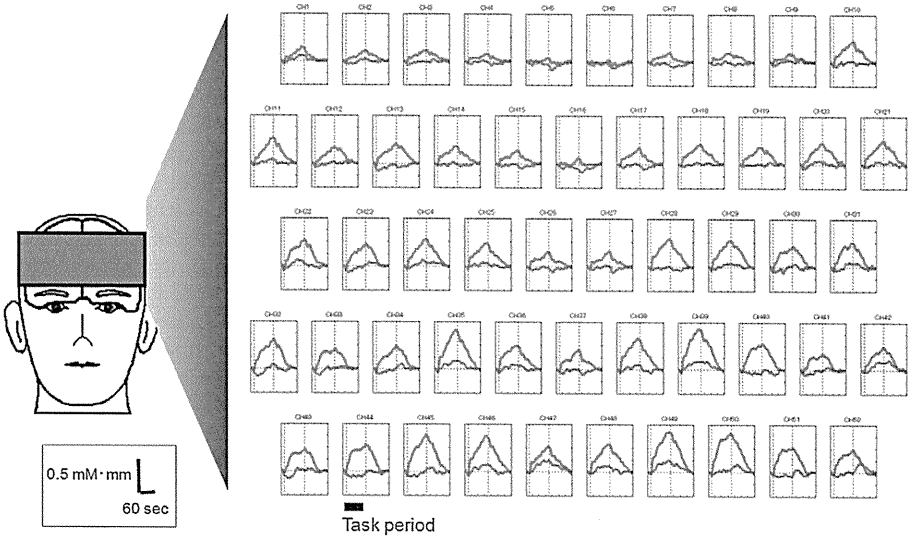

Fig. 2. Grand average waveforms of NIRS signals in patients with schizophrenia and healthy controls during the RNG task. The 52 measuring areas were labelled ch1–ch52 from right-superior to left-inferior sides. This arrangement of the probes can measure haemoglobin concentration changes from the bilateral prefrontal (approximately dorsolateral [Brodmann's area (BA) 9, 46], ventrolateral [BA 44, 45, 47], and frontopolar [BA 10]), and superior temporal cortical surface regions. Oxygenated haemoglobin changes in healthy controls and the patients with schizophrenia during the RNG task were represented as grand average waveforms in 52 channels with red and green lines, respectively. As we got relative waveforms related to task induced activation, we determined pre-task baseline as the mean across last 10 s of the pre-task period and post-task baseline as the mean across last 5 s of the post-task period, and we performed linear fitting on the basis of data between the two baselines. Task period showed between vertical dash lines in boxes, and also indicated a black bar. (For interpretation of the references to colour in this figure legend, the reader is referred to the web version of this article.)

dow: 5 s). Grand mean waveforms averaged across subjects were created separately for each type of [Hb] and for each group. Even when we used these artefact rejection methods, the visible artefact waveforms remained. Thus, we used a computer program, which rejected a channel when there was a visible artefact waveform (Takizawa et al., 2008, 2009). The valid channels varied among participants (schizophrenia: number of channels = 33–52 (mean, 44.7; SD, 10.2); healthy subjects: n = 28–52 (mean, 48.1; SD, 5.1); percentage: schizophrenia, 85.9%; healthy controls, 92.5%, n.s.).

2.4. Statistical analysis

All analyses were performed using Statistical Package for Social Sciences (SPSS) 10.1J (SPSS Inc., Chicago, USA). The recorded haemoglobin data from the counting and activation periods were averaged for each period. In this study, we focussed on [oxy-Hb] because [oxy-Hb] changes can reflect more direct cortical activation than [deoxy-Hb] (Kennan et al., 2002), and is well correlated with Blood-oxygen-level dependence (BOLD) signals of fMRI (Lee et al., 2008; Strangman et al., 2002).

First, for every channel in each group, we compared the mean [oxy-Hb] changes from pre-task baseline to activation period using paired Student's t-test. As we performed 52 paired t-tests, we adopted the false discovery rate (FDR) correction method for correcting the multiple comparisons (two-tailed; we set the value specifying the maximum FDR to 0.05 so that there were no more than 5% false positives on average) (Singh and Dan, 2006). Then, we calculated the effect size (Cohen's d) of the mean [oxy-Hb] changes during the activation period in every channel, for inter-channel comparison to validate the differences among prefrontal cortical sub-regions (Cohen, 1988). Second, we compared the differences and effect size between the patients with schizophrenia and healthy controls during the activation period using Student's t-test (FDR correction method). Finally, we measured the correlation coefficient between the age at onset and [oxy-Hb] changes by Spearman's rank correlation coefficient. We set a significant ρ level to 0.05.

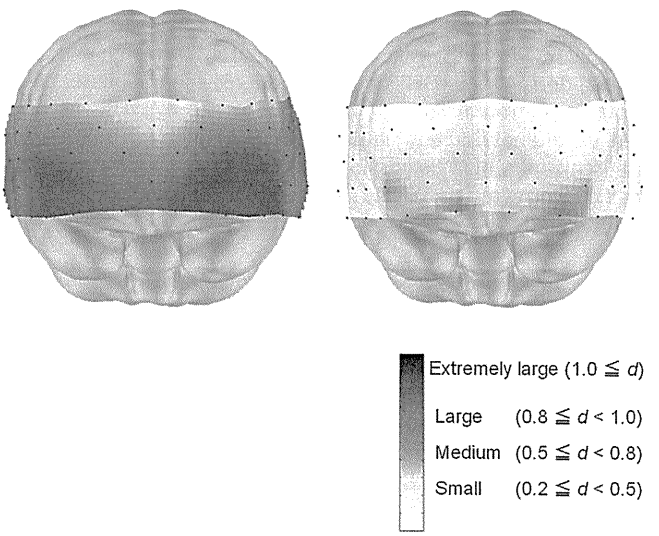

Fig. 3. Topographical 3D mapping of the effect size of [oxy-Hb] changes during the activation period relative to a baseline in control subjects, (left) and patients with schizophrenia (right).

3. Results

RNG task performance (RNG index) was significantly lower in patients with schizophrenia than in healthy controls (p = 0.0497; Table 1).

3.1. [oxy-Hb] changes from counting period to RNG activation period (Fig. 2)

In healthy controls, we found a significant [oxy-Hb] increase in response to performing the RNG task at 44 channels (ch3, 7–8, 10–15, 17–40, 42–50; FDR-corrected p = 0.001–0.038, Fig. 3, left),

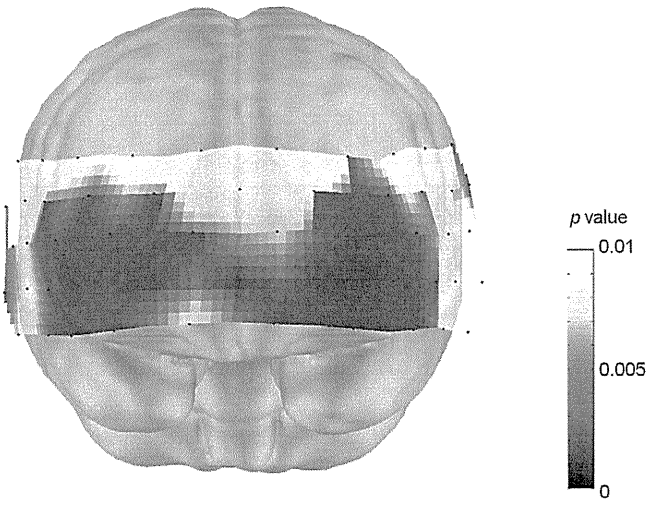

Fig. 4. Topographical 3D mapping of p values from the difference between [oxy-Hb] changes in control and schizophrenia groups. Significant differences are indicated with dark red dots. (For interpretation of the references to colour in this figure legend, the reader is referred to the web version of this article.)

which confirmed significant cognitive activation during the RNG task. The interchannel comparison between counting and activation periods showed the large effect size at 31 channels (ch13–15, 17–19, 21–22, 24–25, 28–32, 34–40, 42, 44–51; d's >0.8, Fig. 3, left), and these channels were located bilaterally in the lateral side of prefrontal regions, compared with those in the frontopolar PFC region. These regions approximately corresponded to the bilateral dorsolateral (DLPFC; BA9 and BA46) and the bilateral ventrolateral prefrontal cortex (VLPFC; BA44, 45, 47). On the other hand, we did not find any significant activation channel in patients with schizophrenia, except for one channel of activation trend (ch49; uncorrected $p = 0.021$, Fig. 3, right).

3.2. Comparison between groups during activation period

The patients with schizophrenia showed significantly smaller activation than the healthy controls during the activation period at 35 channels (ch7, 10–11, 13–15, 17–19, 21, 23–26, 28–40, 43–46, 48–51; FDR-corrected $p = 0.001$–0.029, Fig. 4). The interchannel comparisons of the differences between groups showed large effect size at 23 channels (ch13, 15, 17–19, 21, 24, 28–30, 32, 34–36, 38–40, 44–46, 48–50; d's >0.8), which were approximately located in the bilateral DLPFC and VLPFC regions.

3.3. RNG performance comparison and performance-matched analysis

RNG index was significantly lower in patients with schizophrenia than in healthy controls ($p = 0.0497$; Table 1). Therefore, in a confirmatory analysis, we intended to detect specific haemoglobin changes regardless of the cognitive performances. As we matched RNG task performance between the two groups, we performed a confirmatory analysis in 18 patients with schizophrenia and 33 healthy controls (Schizophrenia: mean RNG index = 0.131 (SD = 0.032); controls: mean = 0.124 (SD = 0.027); $p = 0.42$). The demographic characteristics between the groups remained to be matched for age and gender. In the same manner as the original analysis, the patients with schizophrenia showed significantly reduced activation compared with the healthy controls during the activation period at 32 channels (ch7, 11, 13–15, 17–19, 21–26, 28–29, 32–40, 43–48, 50–51; FDR-corrected $p = 0.001$–0.020).

3.4. Correlation coefficients between NIRS signal changes and onset age

In patients with schizophrenia, four channels in the right DLPFC regions (BA9) showed a significantly positive correlation coefficient with age at onset (ch5: $\rho = 0.607$, $p = 0.003$; ch15: $\rho = 0.584$, $p = 0.005$; ch26: $\rho = 0.544$, $p = 0.013$; ch36: $\rho = 0.522$, $p = 0.015$; Fig. 5), that is, the patients with an earlier onset had smaller [oxy-Hb] changes in the right DLPFC. Their ages at onset were not correlated with any other demographic or clinical variables (age, education, RNG index, any PANSS subscores, GAF score, duration of illness, duration of untreated psychosis and dose of medication). In a confirmatory analysis, even when we divided the schizophrenia group into two subgroups on the basis of median age at onset (median age at onset = 26.0 years; early onset: $n = 10$, mean age at onset = 19.0 years, SD = 3.3; late onset: $n = 12$, mean age at onset = 32.3 years, SD = 7.2), two out of four channels were still significantly different (Ch 15, $p = 0.004$; Ch26, $p = 0.00052$).

4. Discussion

In this study, we investigated haemodynamic changes over PFC during the RNG task using a multichannel NIRS instrument in healthy controls and patients with schizophrenia. Our results showed that bilateral DLPFC and VLPFC activation in healthy controls significantly increased during the RNG task, but did not increase in patients with schizophrenia, even when task performances were matched between groups. Furthermore, the present study showed a significant positive correlation between the age at onset of schizophrenia and their [oxy-Hb] increase in the right DLPFC region (BA 9). In other words, the right DLPFC activations in patients with schizophrenia were poorer when the age at onset was earlier.

4.1. [oxy-Hb] changes due to RNG task

To replicate the previous two-channel NIRS findings, we confirmed a significant [oxy-Hb] increase over the wide area of the PFC in healthy controls associated with the RNG task. In particular, we observed large effect sizes in the bilateral DLPFC and VLPFC regions, suggesting that DLPFC and VLPFC function, rather than other prefrontal cortical function was preferentially recruited when generating random numbers. A previous PET study showed increased activity in the left DLPFC and right inferior frontal cortex (Jahanshahi et al., 2000), and an fMRI study showed increased activation in the bilateral DLPFC in healthy controls during the RNG task (Daniels et al., 2003). It was also implicated in an event-related potential study where the negative component related to random number generation resulted in a maximum negative peak over the left DLPFC region using a low-resolution brain electromagnetic tomography (LORETA) analysis (Joppich et al., 2004). Generating random numbers at a certain time interval demands highly executive processes, attention shifting and inhibition of repetitive attitudes; these functions were mostly related to part of the central executive component included in a working memory model (Artiges et al., 2000; Baddeley and Wilson, 1988; Jahanshahi et al., 2000). Our results support the theory that DLPFC is a major component of the working memory system, and that an NIRS instrument can measure haemodynamic activities in the DLPFC related to the use of working memory.

Our results also showed increased activation in the bilateral VLPFC regions. It has been assumed that VLPFC is also involved in the working memory system (Christ et al., 2009; Dolcos et al., 2007). A previous fMRI study using n-back tasks showed that VLPFC activation, in addition to the DLPFC regions, was increased

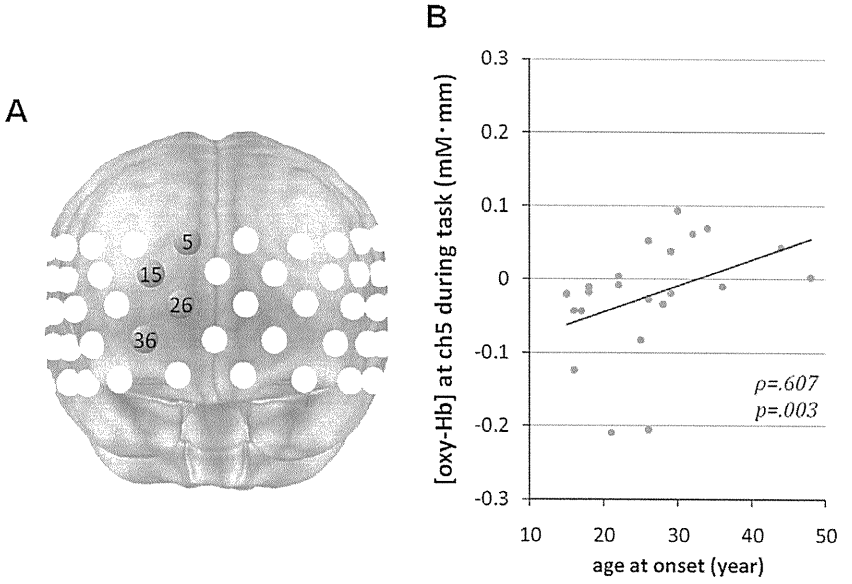

Fig. 5. Relationship between [oxy-Hb] change and age at onset of schizophrenia. (A) The channels which showed significant correlation ($p < 0.05$) are indicated in red. (B) Scatter diagram at ch5 (Spearman's rank correlation coefficient; $\rho = 0.607$, $p = 0.003$). *X* axis shows ages at onset of schizophrenia and *Y* axis shows [oxy-Hb] changes. (For interpretation of the references to colour in this figure legend, the reader is referred to the web version of this article.)

when the participants underwent tasks that demand the maintenance of working memory (Schneider et al., 2007). Therefore, the bilateral VLPFC activation in this study might reflect the need for executive control, inhibition and maintenance of working memory in generating random numbers.

4.2. Group comparison during the RNG task

This study showed that the patients with schizophrenia had significantly smaller activation than the healthy controls over the wide prefrontal cortical regions (35 out of 52 channels), especially in the bilateral DLPFC and VLPFC regions (Fig. 4). Previous two-channel NIRS studies showed significantly reduced [oxy-Hb] changes of the bilateral prefrontal regions during the RNG task in patients with schizophrenia (Hoshi et al., 2006; Shinba et al., 2004). Our multichannel NIRS results replicated the reduced prefrontal activation shown by these two-channel studies and further confirmed the spatial characteristics of prefrontal abnormality in schizophrenia. This reduced activation in schizophrenia may involve decreased capacity of working memory. Recent fMRI studies using working memory tasks have shown that there is an inverted U-curve relationship between DLPFC activation and task difficulty, that is, the activation increased as the task became more difficult up to a certain level, but it decreased when the task level was beyond the capacity of the working memory (Manoach, 2003). An fMRI study in non-psychiatric participants using an RNG task showed that the left DLPFC activation reduced and the right DLPFC activation was absent when the task became difficult (from 1-Hz to faster 2-Hz pacing) (Daniels et al., 2003). In a PET study, healthy volunteers had increased activations in the bilateral DLPFC during slower rate of an RNG task such as 0.5-Hz pacing, and the activation decreased when the pace of response was faster, such as 1-Hz and 2-Hz pacing (Jahanshahi et al., 2000). Furthermore, the task demanded a larger working memory load on patients with schizophrenia than on healthy controls during the same task. Therefore, when comparing the DLPFC activation between patients with schizophrenia and healthy controls, patients with schizophrenia show a relatively larger activation than healthy controls for easy tasks, while showing smaller activation in more difficult tasks (Manoach, 2003). These results suggest that the RNG task using 10 digits and 1-Hz pacing in the present study appeared to be relatively more demanding, even for healthy participants than other working memory tasks, such as Stroop or Sternberg tasks (Daniels et al., 2003). Therefore, our result was in line with previous studies that showed that RNG task with 1-Hz pacing required much working memory load in the healthy controls and resulted in decreased activation in the patients with schizophrenia assuming over their working memory capacity.

4.3. Relationship between oxy-Hb concentration and task performance

The present study showed that the RNG performance in patients with schizophrenia was significantly, although marginally, worse than that of healthy controls, which replicates previous neuropsychological studies (Hoshi et al., 2006; Peters et al., 2007; Shinba et al., 2004). Furthermore, the prefrontal activity (32 out of 52 channels) in the patients with schizophrenia was still significantly reduced compared with healthy controls even when RNG performance was matched. These results suggest that the subtle prefrontal functional abnormality in schizophrenia can be sensitively detected with NIRS, regardless of task performance.

This study did not show any correlation between [oxy-Hb] changes and task performance, while some neuroimaging studies using an RNG task showed a relationship between PFC activation and task performance (Jahanshahi et al., 2000; Shinba et al., 2004). A previous two-channel NIRS study showed that the [oxy-Hb] changes of bilateral frontal regions in healthy controls were positively correlated with task performance during 'written' RNG tasks, but not during 'oral' RNG tasks (Shinba et al., 2004). It has been also shown that activations in the left DLPFC region were positively correlated with task performance in a PET study (Jahanshahi et al., 2000). These studies had a rather small number of participants (13 patients and six healthy controls, respectively), and adopted task procedures and indices of calculating randomness different from our study. Our results limited the high-performance participants who could perform better than 90% accuracy during activation period, which might also have affected the discrepant results. Therefore, the relationship between prefrontal haemodynamic response and task performance during RNG tasks remains

controversial, and further studies using a more sophisticated design and a larger sample may be needed to clarify this point.

4.4. Relationship between age at onset and oxy-Hb concentration changes

The present study using multichannel NIRS showed a significant positive correlation between the age at onset and the [oxy-Hb] changes in four channels (ch5, 16, 26 and 36) located mainly over the right DLPFC region (BA9), regardless of gender, symptom severity, duration of illness or duration of untreated psychosis. Some long-term follow-up studies have suggested that patients with early-onset schizophrenia were associated with severe symptoms and poorer social outcomes (Eggers and Bunk, 1997; Hafner, 2000). A previous neuropsychological study using a verbal learning task showed that subjects with early-onset schizophrenia had worse performance in memory retrieval (Paulsen et al., 1995). Our results indicated more severe DLPFC dysfunction in earlier-onset schizophrenia using functional neuroimaging instruments, which was in accordance with structural MRI studies that showed the relationship between early age at onset and whole-brain-volume reduction (Matsumoto et al., 2001), and severe prefrontal volume loss in early-onset schizophrenia (Thompson et al., 2001).

Trying to delay the onset of schizophrenia is an interesting topic in recent early detection and intervention studies (McGlashan et al., 2006; McGorry et al., 2002). Evidence suggests that prefrontal deficits, including working memory and executive process, existed before schizophrenia onset (Brewer et al., 2005), and delaying and reducing psychosis onset may be possible, though to a limited extent, by using low-dose antipsychotics and/or cognitive behavioural therapy (McGlashan et al., 2006; McGorry et al., 2002). In our next step, we will test whether NIRS instruments may be useful in objectively and easily evaluating the prefrontal dysfunction, selecting the type of intervention and predicting treatment outcome at the ultra-high-risk stage for developing psychosis.

4.5. Limitation

There are some methodological considerations in this study. First, multichannel NIRS has limited spatial resolution compared with fMRI and PET. However, a recent MRI and NIRS combination study, which used a method for the probabilistic registration of NIRS data onto Montreal Neurological Institute (MNI) coordinate space, suggested the errors of spatial estimation, expressed as standard deviations, were approximately 10 mm (Okamoto and Dan, 2005; Tsuzuki et al., 2007). These suggest that multichannel NIRS could roughly detect sub-region-specific activation in the prefrontal cortex. Second, although we did not find any relationships between [oxy-Hb] and duration of illness and medication dosages in the patients with schizophrenia, they were chronic and medicated. Thus, to fully rule out their effects, future studies should evaluate first-episode and/or drug-naïve patients with schizophrenia. Longitudinal assessment of these patients will also overcome the limitation of retrospective assessment of age at onset in this study.

5. Conclusion

In conclusion, our study using multichannel NIRS suggested DLPFC and VLPFC abnormality in patients with schizophrenia during the RNG task. Furthermore, the present study indicated that the severe disturbances of DLPFC functions are correlated with earlier age at onset in schizophrenia. Thus, multichannel NIRS, a non-invasive and easy-to-use instrument, may be useful in evaluating and predicting cognitive function and social outcome in schizophrenia in clinical settings.

Conflict of Interest

None.

Contributors

Author S.K. performed the statistical analyses and wrote the entire article. Authors R.T., K.M., M.K. and Y.K. undertook NIRS measurements. Authors R.T., Y.K., M.R. and K.K. designed the study and wrote the protocol. Author Y.N. managed the literature searches and analyses. All authors contributed to and have approved the final article.

Funding

This study was supported by grants from the Ministry of Health, Labour, and Welfare (Health and Labour Sciences Research Grants, Research on Psychiatric and Neurological Diseases and Mental Health, H19-kokoro-ippan-012, H20-kokoro-ippan-001, and H20-3 to K.K.), and from the JSPS/MEXT (No. 20023009 and 21249064 to K.K.), Japan. A part of this study was also the result of "Development of biomarker candidates for social behavior" carried out under the Strategic Research Program for Brain Sciences by the MEXT.

Acknowledgements

The authors thank all the participants in this study. We also thank Shingo Kawasaki for technical assistance.

References

Addington J, Van Mastrigt S, Addington D. Duration of untreated psychosis: impact on 2-year outcome. Psychol Med 2004;34:277–84.
American Psychiatric Association. Practice guideline for the treatment of patients with schizophrenia. Am J Psychiatry 1997;154:1–63.
American Psychiatric Association. Diagnostic and statistical manual of mental disorders. 4th edition. Washington, DC, USA: American Psychiatric Press; 1994.
Artiges E, Salame P, Recasens C, Poline JB, Attar-Levy D, De La Raillere A, et al. Working memory control in patients with schizophrenia: a PET study during a random number generation task. Am J Psychiatry 2000;157:1517–9.
Baddeley A, Wilson B. Frontal amnesia and the dysexecutive syndrome. Brain Cogn 1988;7:212–30.
Brewer WJ, Francey SM, Wood SJ, Jackson HJ, Pantelis C, Phillips LJ, et al. Memory impairments identified in people at ultra-high risk for psychosis who later develop first-episode psychosis. Am J Psychiatry 2005;162:71–8.
Brugger P, Monsch AU, Salmon DP, Butters N. Random number generation in dementia of the Alzheimer type: a test of frontal executive functions. Neuropsychologia 1996;34:97–103.
Christ SE, Van Essen DC, Watson JM, Brubaker LE, McDermott KB. The contributions of prefrontal cortex and executive control to deception: evidence from activation likelihood estimate meta-analyses. Cereb Cortex 2009;19:1557–66.
Cohen J. Statistical power analysis for the behavioral sciences. 2nd edition. Hillsdayle, New Jersey, USA: Lawrence Erlbaum Associates; 1988.
Daniels C, Witt K, Wolff S, Jansen O, Deuschl G. Rate dependency of the human cortical network subserving executive functions during generation of random number series – a functional magnetic resonance imaging study. Neurosci Lett 2003;345:25–8.
Dolcos F, Miller B, Kragel P, Jha A, McCarthy G. Regional brain differences in the effect of distraction during the delay interval of a working memory task. Brain Res 2007;1152:171–81.
Eggers C, Bunk D. The long-term course of childhood-onset schizophrenia: a 42-year followup. Schizophr Bull 1997;23:105–17.
Evans FJ. Monitoring attention deployment by random number generation: an index to measure subjective randomness. Bull Psychonom Soc 1978;12:35–8.
Fallgatter AJ, Strik WK. Reduced frontal functional asymmetry in schizophrenia during a cued continuous performance test assessed with near-infrared spectroscopy. Schizophr Bull 2000;26:913–9.
First MB, Spitzer RL, Gibbon M, Williams JBW, Kitamura T, Tomita T, et al. Structured clinical interview for DSM-IV axis I disorders (SCID-I). Tokyo, Japan: Nihon Hyoron-Sha Publishers; 2003 [Japanese version].

Ginsburg N, Karpiuk P. Random number generation: analysis of responses. Percept Mot Skills 1994;81:1183–6.
Hafner H. Onset and early course as determinants of the further course of schizophrenia. Acta Psychiatr Scand Suppl 2000:44–8.
Hollingshead AB. Two-factor index of social position. New Haven, USA: Yale University Press; 1965.
Hoshi Y, Shinba T, Sato C, Doi N. Resting hypofrontality in schizophrenia: a study using near-infrared time-resolved spectroscopy. Schizophr Res 2006;84:411–20.
Jahanshahi M, Dirnberger G, Fuller R, Frith CD. The role of the dorsolateral prefrontal cortex in random number generation: a study with positron emission tomography. Neuroimage 2000;12:713–25.
Joppich G, Dauper J, Dengler R, Johannes S, Rodriguez-Fornells A, Munte TF. Brain potentials index executive functions during random number generation. Neurosci Res 2004;49:157–64.
Kakimoto Y, Nishimura Y, Hara N, Okada M, Tanii H, Okazaki Y. Intrasubject reproducibility of prefrontal cortex activities during a verbal fluency task over two repeated sessions using multi-channel near-infrared spectroscopy. Psychiatry Clin Neurosci 2009;63:491–9.
Kay SR, Fiszbein A, Opler LA. The positive and negative syndrome scale (PANSS) for schizophrenia. Schizophr Bull 1987;13:261–76.
Kennan RP, Kim D, Maki A, Koizumi H, Constable RT. Non-invasive assessment of language lateralization by transcranial near infrared optical topography and functional MRI. Hum Brain Mapp 2002;16:183–9.
Kono T, Matsuo K, Tsunashima K, Kasai K, Takizawa R, Rogers MA, et al. Multiple-time replicability of near-infrared spectroscopy recording during prefrontal activation task in healthy men. Neurosci Res 2007;57:504–12.
Kuwabara H, Kasai K, Takizawa R, Kawakubo Y, Yamasue H, Rogers MA, et al. Decreased prefrontal activation during letter fluency task in adults with pervasive developmental disorders: a near-infrared spectroscopy study. Behav Brain Res 2006;172:272–7.
Lee J, Folley BS, Gore J, Park S. Origins of spatial working memory deficits in schizophrenia: an event-related FMRI and near-infrared spectroscopy study. PLoS ONE 2008;3:e1760.
Manoach DS. Prefrontal cortex dysfunction during working memory performance in schizophrenia: reconciling discrepant findings. Schizophr Res 2003;60: 285–98.
Matsumoto H, Simmons A, Williams S, Hadjulis M, Pipe R, Murray R, et al. Superior temporal gyrus abnormalities in early-onset schizophrenia: similarities and differences with adult-onset schizophrenia. Am J Psychiatry 2001;158: 1299–304.
Matsuo K, Onodera Y, Hamamoto T, Muraki K, Kato N, Kato T. Hypofrontality and microvascular dysregulation in remitted late-onset depression assessed by functional near-infrared spectroscopy. Neuroimage 2005;26:234–42.
Matsuo K, Kouno T, Hatch JP, Seino K, Ohtani T, Kato N, et al. A near-infrared spectroscopy study of prefrontal cortex activation during a verbal fluency task and carbon dioxide inhalation in individuals with bipolar disorder. Bipolar Disord 2007;9:876–83.
Matsuo K, Taneichi K, Matsumoto A, Ohtani T, Yamasue H, Sakano Y, et al. Hypoactivation of the prefrontal cortex during verbal fluency test in PTSD: a near-infrared spectroscopy study. Psychiatry Res 2003;124:1–10.
McGlashan TH, Zipursky RB, Perkins D, Addington J, Miller T, Woods SW, et al. Randomized, double-blind trial of olanzapine versus placebo in patients prodromally symptomatic for psychosis. Am J Psychiatry 2006; 163:790–9.
McGorry PD, Yung AR, Phillips LJ, Yuen HP, Francey S, Cosgrave EM, et al. Randomized controlled trial of interventions designed to reduce the risk of progression to first-episode psychosis in a clinical sample with subthreshold symptoms. Arch Gen Psychiatry 2002;59:921–8.
Nishimura Y, Tanii H, Fukuda M, Kajiki N, Inoue K, Kaiya H, et al. Frontal dysfunction during a cognitive task in drug-naive patients with panic disorder as investigated by multi-channel near-infrared spectroscopy imaging. Neurosci Res 2007;59:107–12.
Okada E, Delpy DT. Near-infrared light propagation in an adult head model. II. Effect of superficial tissue thickness on the sensitivity of the near-infrared spectroscopy signal. Appl Opt 2003;42:2915–22.
Okamoto M, Dan I. Automated cortical projection of head-surface locations for transcranial functional brain mapping. Neuroimage 2005;26:18–28.
Oldfield RC. The assessment and analysis of handedness: the Edinburgh inventory. Neuropsychologia 1971;9:97–113.
Otsubo T, Tanaka K, Koda R, Shinoda J, Sano N, Tanaka S, et al. Reliability and validity of Japanese version of the Mini-International Neuropsychiatric Interview. Psychiatry Clin Neurosci 2005;59:517–26.
Paulsen JS, Heaton RK, Sadek JR, Perry W, Delis DC, Braff D, et al. The nature of learning and memory impairments in schizophrenia. J Int Neuropsychol Soc 1995;1:88–99.
Peters M, Giesbrecht T, Jelicic M, Merckelbach H. The random number generation task: psychometric properties and normative data of an executive function task in a mixed sample. J Int Neuropsychol Soc 2007;13:626–34.
Schneider F, Habel U, Reske M, Kellermann T, Stocker T, Shah NJ, et al. Neural correlates of working memory dysfunction in first-episode schizophrenia patients: an fMRI multi-center study. Schizophr Res 2007;89:198–210.
Shinba T, Nagano M, Kariya N, Ogawa K, Shinozaki T, Shimosato S, et al. Near-infrared spectroscopy analysis of frontal lobe dysfunction in schizophrenia. Biol Psychiatry 2004;55:154–64.
Singh AK, Dan I. Exploring the false discovery rate in multichannel NIRS. Neuroimage 2006;33:542–9.
Spatt J, Goldenberg G. Components of random generation by normal subjects and patients with dysexecutive syndrome. Brain Cogn 1993;23:231–42.
Strangman G, Culver JP, Thompson JH, Boas DA. A quantitative comparison of simultaneous BOLD fMRI and NIRS recordings during functional brain activation. Neuroimage 2002;17:719–31.
Suto T, Fukuda M, Ito M, Uehara T, Mikuni M. Multichannel near-infrared spectroscopy in depression and schizophrenia: cognitive brain activation study. Biol Psychiatry 2004;55:501–11.
Takizawa R, Kasai K, Kawakubo Y, Marumo K, Kawasaki S, Yamasue H, et al. Reduced frontopolar activation during verbal fluency task in schizophrenia: a multi-channel near-infrared spectroscopy study. Schizophr Res 2008;99:250–62.
Takizawa R, Tochigi M, Kawakubo Y, Marumo K, Sasaki T, Fukuda M, et al. Association between catechol-O-methyltrasferase Val108/158Met genotype, prefrontal hemodynamic response in schizophrenia. PLoS ONE 2009;4:e5495.
Thompson PM, Vidal C, Giedd JN, Gochman P, Blumenthal J, Nicolson R, et al. Mapping adolescent brain change reveals dynamic wave of accelerated gray matter loss in very early-onset schizophrenia. Proc Natl Acad Sci USA 2001;98:11650–5.
Tsuzuki D, Jurcak V, Singh AK, Okamoto M, Watanabe E, Dan I. Virtual spatial registration of stand-alone fNIRS data to MNI space. Neuroimage 2007;34: 1506–18.
Watanabe E, Yamashita Y, Maki A, Ito Y, Koizumi H. Non-invasive functional mapping with multi-channel near infra-red spectroscopic topography in humans. Neurosci Lett 1996;205:41–4.
Yamashita Y, Maki A, Ito Y, Watanabe E, Koizumi H. Noninvasive near-infrared topography of human brain activity using intensity modulation spectroscopy. Opt Eng 1996;35:1046–9.

Contents lists available at ScienceDirect

Progress in Neuro-Psychopharmacology & Biological Psychiatry

journal homepage: www.elsevier.com/locate/pnp

A polymorphism of the *ABCA1* gene confers susceptibility to schizophrenia and related brain changes

Miho Ota [a,*,1], Takashi Fujii [a,1], Kiyotaka Nemoto [b,c], Masahiko Tatsumi [d], Yoshiya Moriguchi [c], Ryota Hashimoto [a,e,f], Noriko Sato [c], Nakao Iwata [g,h], Hiroshi Kunugi [a]

[a] *Department of Mental Disorder Research, National Institute of Neuroscience, National Center of Neurology and Psychiatry, 4-1-1 Ogawa-Higashi, Kodaira, Tokyo 187-8502, Japan*
[b] *Division of Psychiatry, Tsukuba University Hospital, 2-1-1 Amakubo, Tsukuba, Ibaraki 305-8576, Japan*
[c] *Department of Radiology, National Center of Neurology and Psychiatry, 4-1-1, Ogawa-Higashi, Kodaira, Tokyo 187-8551, Japan*
[d] *Yokohama Shinryo Clinic, Yokohama 221-0835, Japan*
[e] *Molecular Research Center for Children's Mental Development, United Graduate School of Child Development, Osaka University, Kanazawa University and Hamamatsu University School of Medicine, D3, 2-2, Yamadaoka, Suita, Osaka, 565-0871, Japan*
[f] *Department of Psychiatry, Osaka University Graduate School of Medicine, D3, 2-2, Yamadaoka, Suita, Osaka, 565-0871, Japan*
[g] *Department of Psychiatry, School of Medicine, Fujita Health University, Toyoake, Aichi, Japan*
[h] *Japan Science and Technology Agency, the Core Research for Evolutional Science and Technology, Kawaguchi, Japan*

ARTICLE INFO

Article history:
Received 14 April 2011
Received in revised form 14 July 2011
Accepted 26 July 2011
Available online 3 August 2011

Keywords:
ATP-binding cassette transporter A1
Polymorphism
Schizophrenia
Voxel based morphometry

ABSTRACT

Objective: The ATP-binding cassette transporter A1 (ABCA1) mediates cellular cholesterol efflux through the transfer of cholesterol from the inner to the outer layer of the cell membrane and regulates extracellular cholesterol levels in the central nervous system. Several lines of evidence have indicated lipid and myelin abnormalities in schizophrenia.
Method: Initially, we examined the possible association of the polymorphisms of the ABCA1 gene (*ABCA1*) with susceptibility to schizophrenia in 506 patients with schizophrenia (DSM-IV) and 941 controls. The observed association was then subject to a replication analysis in an independent sample of 511 patients and 539 controls. We further examined the possible effect of the risk allele on gray matter volume assessed with magnetic resonance imaging (MRI) in 86 patients with schizophrenia (49 males) and 139 healthy controls (47 males).
Results: In the initial association study, the 1587 *K* allele (rs2230808) was significantly more common in male patients with schizophrenia than in male controls. Although such a significant difference was not observed in the second sample alone, the increased frequency of the 1587 K allele in male patients remained to be significant in the combined male sample of 556 patients and 594 controls. Male schizophrenia patients carrying the 1587 *K* allele had a smaller amount of gray matter volume than those who did not carry the allele.
Conclusion: Our data suggest a male-specific association of the 1587 *K* allele of *ABCA1* with susceptibility to schizophrenia and smaller gray matter volume in schizophrenia.

1. Introduction

The ATP-binding cassette transporter A1 (ABCA1) mediates cellular cholesterol efflux through transfer of cholesterol from the inner to the outer layer of the cell membrane, enabling the binding of cholesterol to apolipoproteins (Knight, 2004). It plays a critical role in the regulation of extracellular cholesterol levels in the central nervous system (CNS). Mice lacking the ABCA1 gene (*ABCA1*) had significantly reduced cholesterol levels in the cerebrospinal fluid (Wahrle et al., 2004). Moreover, *ABCA1* polymorphisms are reported to be associated with serum cholesterol concentration. For instance, the 219*K* (rs2230806) allele was associated with high plasma levels of low-density lipoprotein (LDL) cholesterol (Katzov et al., 2004), and the 771*M* (rs2066718) and the 1587*K* (rs2230808) alleles were associated with low plasma levels of high-density lipoprotein (HDL) cholesterol (Clee et al., 2001; Frikke-Schmidt et al., 2004). Cholesterol is required for myelination (Saher

Abbreviations: ABCA1, ATP-binding cassette transporter A1; ANCOVA, analysis of covariance; ANOVA, analysis of variance; CNS, central nervous system; DNA, deoxyribonucleic acid; DSM-IV, Diagnostic and Statistical Manual of Mental Disorders, 4th edition; FDR, false discovery rate; FWE, familywise error rate; GWAS, genome-wide association study; HDL, high-density lipoprotein; HWE, Hardy–Weinberg equilibrium; IL1β, interleukin-1 β; LDL, low-density lipoprotein; MINI, Mini-International Neuropsychiatric Interview; MRI, magnetic resonance imaging; mRNA, messenger ribonucleic acid; PCR, polymerase chain reaction; SNP, single nucleotide polymorphisms; SPM, Statistical Parametric Mapping; TE, echo time; TR, repetition time; VBM, voxel-based morphometry

* Corresponding author. Tel.: +81 42 341 2712; fax: +81 42 346 2094.
E-mail address: ota@ncnp.go.jp (M. Ota).
[1] Contributed equally to this work.

0278-5846/$ – see front matter © 2011 Elsevier Inc. All rights reserved.
doi:10.1016/j.pnpbp.2011.07.012

et al., 2005), dendrite differentiation (Goritz et al., 2005) and synaptogenesis (Mauch et al., 2001). Therefore ABCA1 expressed in neurons and glial cells plays an important role in the regulation of synaptic development (Karasinska et al., 2009). Estrogen administration is also known to increase *ABCA1* messenger ribonucleic acid (mRNA) (Srivastava, 2002), and a sex difference in the activity of cholesterol transport has been observed (Catalano, 2008). Disturbances in CNS cholesterol homeostasis have been implicated in neurodegenerative diseases including Alzheimer's (Vance et al., 2005) and Huntington's diseases (Valenza et al., 2005). Previous studies have examined the association between polymorphisms of *ABCA1*, particularly the non-synonymous single nucleotide polymorphisms (SNPs) of rs2230806 (*R219K*), rs2066718 (*V771M*), and rs2230808 (*R1587K*) and risk for Alzheimer's disease. Some of these studies have shown a significant association (Katzov et al., 2004; Sundar et al., 2007; Shibata et al., 2006), although this association demonstrated a sex difference (Sundar et al., 2007). Several studies have demonstrated myelin abnormalities in schizophrenia (Thomas et al., 2001; Hakak et al., 2001; Garver et al., 2008; Tkachev et al., 2003; Huang and Chen, 2005), and the relationship between schizophrenia and ABCA1 was also noted (Chen et al., 2009). To date, sterol-regulatory-element binding protein-2 (SREBP-2), that regulates the ABCA1 (Wong et al., 2006), was suggested to be associated with schizophrenia (Le Hellard et al., 2010). Recent genetic studies also have revealed that the interleukin-1 β (IL1β) gene or the IL1 gene complex is associated with schizophrenia (Xu and He, 2010), and it is also suggested that change in IL1β levels in cerebrospinal fluid and serum may play a role in the pathophysiology of schizophrenia (Barak et al., 1995). IL-1β has been shown to down-regulate ABCA1 (Chen et al., 2007). However, to our knowledge, no study has thus far focused on the association between *ABCA1* polymorphisms and risk of schizophrenia. To our knowledge, no genome-wide association study (GWAS) has suggested that this chromosomal region contains a susceptibility locus for schizophrenia yet. However, some GWASs for bipolar disorder have reported this locus as a candidate region. Data from GWASs are also beginning to provide strong support for shared genetic risk across the disorders (Venken et al., 2005; Park et al., 2004; Liu et al., 2003; Badenhop et al., 2002). Interestingly, a recent study using data from GWASs strongly supported the hypothesis of shared genetic risk between schizophrenia and bipolar disorder (Moskvina et al., 2009). Thus we examined the possibility of association between the *ABCA1* variants and schizophrenia.

Previous magnetic resonance imaging (MRI) studies in schizophrenia have shown gray matter volume reduction, particularly in the insula, anterior cingulate cortex, medial frontal cortex, and hippocampal area (Fornito et al., 2009; Glahn et al., 2008). Furthermore, studies have shown the effect of disease-associated genes on such structural abnormalities in the brain (Mata et al., 2009). Deviations in brain morphology potentially reflecting genetic risk have been ubiquitous in the literature, and quantitative measures of brain structure using various neuroimaging techniques have a long history as effective endophenotype (Honea et al., 2008). In this study, we examined whether genetic variations of *ABCA1* are associated with the development of schizophrenia. We also investigated the potential influence of the disease-associated genotype of *ABCA1* on the regional cerebral gray matter volume measured with MRI.

2. Methods

2.1. Subjects

2.1.1. Initial study (Tokyo sample)

Subjects were 506 patients with schizophrenia (278 males, mean age 44.3 ± 14.1 years), diagnosed according to the Diagnostic and Statistical Manual of Mental Disorders, 4th edition (DSM-IV) (American Psychiatric Association, 1994), and 941 healthy controls (334 males, 44.8 ± 16.3 years). All patients and controls were biologically unrelated Japanese who resided in the same geographical area (the western part of Tokyo). Consensus diagnosis by at least two psychiatrists was made for each patient based on all the available information obtained from interviews and medical records. Healthy controls were interviewed for enrollment by research psychiatrists using the Japanese version of the Mini-International Neuropsychiatric Interview (MINI; Otsubo et al., 2005; Sheehan et al., 1998). Those who demonstrated no history of psychiatric illness or contact with psychiatric services were enrolled as controls in this study. Participants were excluded if they had a prior medical history of CNS disease or severe head injury. Among the subjects, 86 (49 males) schizophrenia patients and 139 healthy controls (47 males) underwent brain MRI.

2.1.2. Replication study (Tokai sample)

For the replication analysis, we used an independent Japanese sample comprising 511 cases (283 males, mean age 43.8 ± 14.9 years) and 539 controls (267 males, 36.3 ± 14.2 years). All subjects were unrelated, living in the Tokai area of the mainland of Japan, and self-identified as Japanese. Control subjects were members of the general public who had no personal history of mental disorders. This was ascertained in face-to-face interviews where subjects were asked if they had suffered an episode of depression, mania, or psychotic experiences or if they had received treatment for any psychiatric disorder. Patients were entered into the study if they 1) met DSM-IV criteria for schizophrenia; 2) were physically healthy and had normal routine laboratory tests; and 3) had no mood disorders, substance abuse, neurodevelopmental disorders, epilepsy, or known mental retardation. Consensus diagnoses were made by at least two experienced psychiatrists according to DSM-IV criteria on the basis of unstructured interviews with patients and families and review of medical records.

After description of the study, written informed consent was obtained from each subject. This study was approved by institutional ethics committees.

2.2. SNP selection and genotyping

Since genetic variations that result in an amino acid change are most likely to alter function, we searched for non-synonymous polymorphisms of *ABCA1* in the NCBI dbSNP database (http://www.ncbi.nlm.nih.gov/sites/entrez?db=snp). We also searched the literature for polymorphisms of *ABCA1* previously reported to be associated with CNS diseases. We found only four well-validated SNPs with a heterozygosity value of >0.10 in Asian populations: rs2230806 (*R219K*), rs2066718 (*V771M*), rs2066714 (*I883M*), and rs2230808 (*R1587K*). Venous blood was drawn from the subjects and genomic deoxyribonucleic acid (DNA) was extracted from whole blood according to the standard procedures. The four SNPs were genotyped using the TaqMan 5′-exonuclease allelic discrimination assay; the assay IDs were C___2741051_1_ for rs2230806, C__11720789_10 for rs2066718, C___2741083_1_ for rs2066714, and C___2741104_1_ for rs2230808 (Applied Biosystems, Foster City, CA). Thermal cycling conditions for polymerase chain reaction (PCR) were 1 cycle at 95 °C for 10 min followed by 50 cycles of 92 °C for 15 s and 60 °C for 1 min. After amplification, the allele-specific fluorescence was measured on ABI PRISM 7900 Sequence Detection (Applied Biosystems). The genotypes were scored using the software SDS2.1. Failed reactions were called as 'undetermined' by this one and these data were not included in the analysis. Genotype data were read blind to the case–control status.

2.3. MRI data acquisition and processing

All MR studies were performed on a 1.5 Tesla Siemens Magnetom Vision plus system. A three-dimensional (3D) volumetric acquisition of a T1-weighted gradient echo sequence produced a gapless series of 144 sagittal sections using an MPRAGE sequence (echo time (TE)/repetition time (TR): 4.4/11.4 ms; flip angle: 15°; acquisition

matrix: 256×256; 1NEX, field of view: 31.5 cm; slice thickness: 1.23 mm). The raw 3D T1-weighted volume data were transferred to a workstation, and structural images were analyzed using an optimized, voxel-based morphometry (VBM) technique. Data were analyzed using Statistical Parametric Mapping 5 (SPM5) software (Welcome Department of Imaging Neuroscience, London, UK) running on MATLAB 7.0 (Math Works, Natick, MA). Images were processed using an optimized VBM script. The details of this process are described elsewhere (Li and Ji, 2005). First, each individual 3D-T1 image was normalized with the optimized VBM method. Normalized segmented images were modulated by multiplication with Jacobian determinants of the spatial normalization function to encode the deformation field for each subject as tissue density changes in normal space. Images were smoothed using an 8-mm full-width at half-maximum of an isotropic Gaussian kernel.

2.4. Statistical analysis

Deviations of genotype distributions from the Hardy–Weinberg equilibrium (HWE) were assessed with the χ^2 test for goodness of fit. First, genotype distributions were compared between patients and controls using the χ^2 test for independence. Since some animal studies showed the gender specific findings (Koldamova et al., 2005; Kuivenhoven et al., 2003), and estrogen has functional relevance to the *ABCA1*-mediated pathway (Srivastava, 2002) and a sex difference in the activity of cholesterol transport has been observed (Catalano et al., 2008), analysis for each sex was also performed. These tests were performed with SPSS software ver. 11 (SPSS Japan, Tokyo, Japan). For multiple analyses, we applied the spectral decomposition method of SNPSpD software (http://gump.qimr.edu.au/general/daleN/SNPSpD/) (Nyholt, 2004; Li and Ji, 2005), which considers marker linkage disequilibrium information and generates an experiment-wide significance threshold required to keep the type I error rate at 5%. As a result, the critical P value was corrected as 0.0128. Then, the observed association was subject to a replication analysis in an independent Tokai sample using the χ^2 test for independence.

Second, we then evaluated the differences in regional gray matter volume across the clusters sorted by the genotype distributions of the SNP that showed a statistically significant difference between the patients and healthy subjects. Statistical analyses were performed using Statistical Parametric Mapping 2 (SPM2) software (Welcome Department of Imaging Neuroscience, London, UK). Since the regional cerebral gray matter volume is influenced by age (Good et al., 2001), we examined the differences in regional gray matter volume by the analysis of covariance (ANCOVA), controlling for age. Only associations that met the following criteria were deemed statistically significant for the first analysis: familywise error rate (FWE)<0.05, and for the *post hoc* analyses: a voxel level of $p<0.001$ (uncorrected) and a cluster level of $p<0.05$ (uncorrected). We also evaluated the differences across the groups according to age using one-way analysis of variance (ANOVA) and the differences between two groups of schizophrenia patients categorized according to duration of illness and daily dose of antipsychotic drugs using a two-sample *t*-test.

3. Results

3.1. ABCA1 polymorphisms and susceptibility to schizophrenia

First, genotype and allele distributions of the 4 SNPs in the initial sample (Tokyo sample) are shown in Table 1. The genotype distribution for rs2230806 in the female control group deviated significantly from the HWE, thus was excluded from further analysis. In the total sample, the genotype or allele distribution did not differ significantly between the cases and controls for any SNP. However, when men and women were examined separately, a nominally significant difference in the genotype distribution for rs2230808 (*R1587K*) was observed in men ($p=0.014$), but not in women ($p=0.674$). Difference in allele frequency was observed at a trend level in men ($p=0.055$), but not in women ($p=0.440$). When the observed difference in the genotype distribution for rs2230808 was further analyzed based on the recessive and dominant models, there was a significant difference in the dominant model ($p=0.006$; odds ratio (OR) 1.60, 95% confidential interval (CI): 1.14–2.24), but not in the recessive one ($p=0.96$), in male subjects. There was no significant difference in genotype or allele distribution of the other 3SNPs even when subjects were stratified by sex.

Table 2 shows genotype and allele distributions for rs2230808 in the replication sample (Tokai sample). There was no significant difference in genotype or allele distribution between the patients and controls. When men and women were examined separately, there was no significant difference for either sex. We also analyzed based on the dominant model; however, no statistically significant differences in genotype distribution were found in total subjects or each sex. However, the initial and replication samples were combined, the frequency of male patients carrying the 1587K allele remained to be increased than male controls at nominally significant level (OR 1.30, 95% CI 1.02 –1.65, $p=0.032$).

3.2. ABCA1 polymorphism and MRI volumetry

Since carrying the 1587*K* allele was found to be significantly more common in male patients with schizophrenia than in male controls in the genetic association study, the subjects with MRI data were grouped into four groups for each sex based on the case-control status and whether the subject carried the 1587*K* allele or not. The demographic and clinical characteristics of the groups are presented in Table 3. For both men and women, the analyses showed no significant difference in duration of illness or daily dose of antipsychotics between the two genotype-based groups of patients with schizophrenia (men: duration of illness: $t(47)=-0.15$, $p=0.88$, daily dose of drug: $t(47)=-1.58$, $p=0.12$; female: duration of illness: $t(34)=-0.40$, $p=0.69$, daily dose of drug: $t(34)=-0.20$, $p=0.85$). Further, for both men and women, there was no significant difference in mean age across the healthy subjects and two schizophrenia groups (men: $df=2$, $F=1.54$, $p=0.22$; women: $df=2$, $F=1.16$, $p=0.32$).

Initially, we evaluated the difference in gray matter volume between the two genotype-based healthy groups for each sex using ANCOVA, controlling for age. There were no significant differences related to genotype for either sex, respectively. We therefore combined the healthy groups with and without the 1587*K* allele for each sex in the following analyses. When the group effect was assessed using ANCOVA with F-test (FWE<0.05), we found statistically significant volume differences in thalami, medial temporal regions, and nearly all the circumferential cortical regions in males (Fig. 1A). Male patients with schizophrenia carrying the 1587*K* allele showed significant small gray matter volume in the bilateral occipital regions and posterior cingulate cortices compared with those who did not carry the 1587*K* allele (Fig. 1B). Male patients with schizophrenia who did not carry the 1587*K* allele showed significant small volume only in bilateral orbitofrontal, insulae, and left parahippocampus, compared with all male controls (Fig. 1C). However, the male schizophrenia patients carrying the 1587*K* allele showed smaller volume across almost the whole gray matter, than all male controls (Fig. 1D). When we re-analyzed these *post hoc* statistics using rigorous criteria (false discovery rate (FDR) $p<0.05$, cluster level of $p<0.05$), results indicated with Fig. 1C and D showed almost the same as the previous ones, the statistics using the relatively small sample size indicated with the Fig. 1B showed no statistically significant difference between the schizophrenic groups.

In women, in contrast, there were no significant differences in gray matter volume between schizophrenia patients with and without the 1587*K* allele or between controls with and without the allele (data not

Table 1
Genotype and allelic distributions of the ABCA1 SNPs in patients with schizophrenia and controls.

db SNP ID and aminoacid change	Position*	Inter-SNP distance (bp)	Gender	Group	N	Genotype distribution (frequency)			$\chi 2$	P	Allele count (frequency)				$\chi 2$	P	HWE of Controls (df = 1)
						R/R	*R/K*	*K/K*			*R*		*K*				
rs2230806 Arg219Lys	107620867 exon 7	(–)	All	Schizophrenia	497	119 (0.24)	241 (0.48)	137 (0.28)	2.77	0.250	479	(0.48)	515	(0.52)	0.01	0.897	$\chi^2 = 3.73$
				Controls	932	204 (0.22)	495 (0.53)	233 (0.25)			903	(0.48)	961	(0.52)			P = 0.053
			M	Schizophrenia	274	63 (0.23)	137 (0.50)	74 (0.27)	0.47	0.789	263	(0.48)	285	(0.52)	0.45	0.503	$\chi^2 = 0.05$
				Controls	330	71 (0.22)	162 (0.49)	97 (0.29)			304	(0.46)	356	(0.54)			P = 0.827
			F	Schizophrenia	223	56 (0.25)	104 (0.47)	63 (0.28)			216	(0.48)	230	(0.52)			$\chi^2 = 6.81$
				Controls	602	133 (0.22)	333 (0.55)	136 (0.23)			599	(0.50)	605	(0.50)			P = 0.009
						V/V	*V/M*	*M/M*			*V*		*M*				
rs2066718 Val771Met	107589255 exon 16	31,612	All	Schizophrenia	494	438 (0.89)	54 (0.11)	2 (0.00)	1.09	0.580	930	(0.94)	58	(0.06)	0.99	0.319	$\chi^2 = 0.04$
				Controls	936	812 (0.87)	120 (0.13)	4 (0.00)			1744	(0.93)	128	(0.07)			P = 0.847
			M	Schizophrenia	273	242 (0.89)	29 (0.11)	2 (0.01)	1.70	0.428	513	(0.94)	33	(0.06)	0.50	0.480	$\chi^2 = 0.30$
				Controls	333	287 (0.86)	45 (0.14)	1 (0.00)			619	(0.93)	47	(0.07)			P = 0.582
			F	Schizophrenia	221	196 (0.89)	25 (0.11)	0 (0.00)	1.32	0.518	417	(0.94)	25	(0.06)	0.60	0.437	$\chi^2 = 0.03$
				Controls	603	525 (0.87)	75 (0.12)	3 (0.00)			1125	(0.93)	81	(0.07)			P = 0.856
						I/I	*I/M*	*M/M*			*I*		*M*				
rs2066714 Ile883Met	107586753 exon 18	34,114	All	Schizophrenia	487	208 (0.43)	212 (0.44)	67 (0.14)	3.86	0.145	628	(0.64)	346	(0.36)	1.75	0.186	$\chi^2 = 0.91$
				Controls	917	345 (0.38)	446 (0.49)	126 (0.14)			1136	(0.62)	698	(0.38)			P = 0.339
			M	Schizophrenia	266	115 (0.43)	116 (0.44)	35 (0.13)	3.23	0.199	346	(0.65)	186	(0.35)	0.87	0.335	$\chi^2 = 2.40$
				Controls	330	122 (0.37)	168 (0.51)	40 (0.12)			412	(0.62)	248	(0.38)			P = 0.122
			F	Schizophrenia	221	93 (0.42)	96 (0.43)	32 (0.14)	1.23	0.542	282	(0.64)	160	(0.36)	0.62	0.430	$\chi^2 = 0.002$
				Controls	587	223 (0.38)	278 (0.47)	86 (0.15)			724	(0.62)	450	(0.38)			P = 0.966
						R/R	*R/K*	*K/K*			*R*		*K*				
rs2230808 Arg1587Lys	107562804 exon 35	58,063	All	Schizophrenia	491	174 (0.35)	252 (0.51)	65 (0.13)	4.05	0.132	600	(0.61)	382	(0.39)	0.63	0.427	$\chi^2 = 0.50$
				Controls	923	367 (0.40)	422 (0.46)	134 (0.15)			1156	(0.63)	690	(0.37)			P = 0.478
			M	Schizophrenia	273	87 (0.32)	148 (0.54)	38 (0.14)	8.51	0.014	322	(0.59)	224	(0.41)	3.68	0.055	$\chi^2 = 1.17$
				Controls	327	140 (0.43)	141 (0.43)	46 (0.14)			421	(0.64)	233	(0.36)			P = 0.278
			F	Schizophrenia	218	87 (0.40)	104 (0.48)	27 (0.12)	0.79	0.674	278	(0.64)	158	(0.36)	0.60	0.440	$\chi^2 = 0.01$
				Controls	596	227 (0.38)	281 (0.47)	88 (0.15)			735	(0.62)	457	(0.38)			P = 0.945

HWE; Hardy–Weinberg equilibrium.
* Chromosome position was determined from the dbSNP database.

Table 2
Genotype and allelic distributions of rs2230808 in independent replication sample.

db SNP ID and aminoacid change	Gender	Group	N	Genotype distribution (frequency)			$\chi 2$	P	Allele count (frequency)				$\chi 2$	P	HWE of controls (df = 1)
				R/R	*R/K*	*K/K*			*R*		*K*				
rs2230808 Arg1587Lys	All	Schizophrenia	539	211 (0.39)	252 (0.47)	76 (0.14)	0.25	0.88	676	(0.63)	404	(0.37)	0.03	0.85	$\chi^2 = 0.49$
		Controls	511	201 (0.39)	233 (0.46)	77 (0.15)			635	(0.62)	387	(0.38)			P = 0.48
	M	Schizophrenia	283	109 (0.39)	133 (0.47)	41 (0.14)	0.15	0.93	351	(0.62)	215	(0.38)	0.14	0.71	$\chi^2 = 0.01$
		Controls	267	106 (0.40)	125 (0.47)	36 (0.13)			337	(0.63)	197	(0.37)			P = 0.92
	F	Schizophrenia	256	102 (0.40)	119 (0.46)	35 (0.14)	0.97	0.62	323	(0.63)	189	(0.37)	0.43	0.51	$\chi^2 = 1.17$
		Controls	244	95 (0.39)	108 (0.44)	41 (0.17)			298	(0.61)	190	(0.39)			P = 0.28

HWE; Hardy–Weinberg equilibrium.

shown). We evaluated the difference between the all controls and all cases using ANCOVA. The female schizophrenia patients showed smaller gray matter volume in the bilateral insulae, anterior cingulate cortex, and orbitofrontal cortex, than all female controls (Fig. 1E).

We also we evaluated the difference in gray matter volume between the schizophrenic groups with and without the 1587*K* allele for each sex using ANCOVA, controlling for age, duration of illness, educational period, and medication. There were no statistically significant differences between the groups for each sex, however, male patients with schizophrenia carrying the 1587*K* allele showed small gray matter volume in the left occipital region and bilateral posterior cingulate cortices, almost the same as Figure (B), compared with those who did not carry the 1587*K* allele at nominal trend level (F) ($P<0.01$ uncorrected). There were no differences between the female schizophrenic patients with or without the 1587*K* allele using loose criteria ($P<0.01$ uncorrected, data not shown).

4. Discussion

We found that the 1587*K* allele of *ABCA1* was significantly more common in male patients with schizophrenia than in male controls. However, such a difference was not observed in women. Furthermore, our results showed that male schizophrenic patients who carried the 1587*K* allele have smaller gray matter volume than in those who did not, but this difference did not extend to women. To our knowledge, this is the first study that reports the possible association of *ABCA1* with susceptibility to schizophrenia and related brain abnormalities.

4.1. ABCA1 polymorphisms and susceptibility to schizophrenia

The 1587*K* allele was reported to increase cerebrospinal fluid tau level and brain amyloid beta load (Katzov et al., 2004). It was also associated with low plasma levels of apolipoprotein A1 (Tregouet et al., 2004) and HDL-cholesterol (Clee et al., 2001; Frikke-Schmidt et al., 2004), suggesting functional differences between the *R*1587 and 1587*K* alleles, which may explain our results.

The present study showed gender-specific association between *R*1587*K* (rs2230808) and schizophrenia in our population. Serum from men displays an enhanced free cholesterol efflux capacity via the ABCA1 transporter pathway compared with that from perimenopausal women (Catalano et al., 2008). Estradiol was known to modulate a wide range of functions of the brain. From the onset of menopause, declining levels of estradiol can cause cognitive disturbances and changes in behavior that can be counterbalanced by hormone replacement. Studies in mice have suggested that the atheroprotective effects of estrogen may occur partly via the ABCA1-mediated pathway (Srivastava, 2002). Another study found that ABCA1 was up-regulated by estradiol (Sárvári et al., 2010). Taking these previous findings into consideration, the observed sex difference in our study may be explained, at least in part, by the fact that estrogen is involved in the regulation of ABCA1 activity. The role of CNS cholesterol in synaptic function and neurodegenerative disorders has recently been appreciated, but the mechanisms regulating its transport and homeostasis are only partially understood. Therefore, further studies that focused on the sex difference should be needed to reveal the function of the ABCA1.

In the initial study, the 1587*K* allele (rs2230808) was significantly more common in male patients with schizophrenia than in male controls. Although such a significant difference was not observed in the second sample alone, the increased frequency of the 1587K allele in male patients remained to be significant in the combined male sample. Though there was the association of *ABCA1* with susceptibility to schizophrenia, it is suggested that this relationship may be fairly weak.

4.2. ABCA1 polymorphism and MRI volumetry

Our results showed that male schizophrenia patients carrying the 1587*K* allele showed smaller gray matter volume than those who did not carry the allele. Schizophrenia has been associated with volume reductions in the limbic, paralimbic, frontal, and temporal cortical regions (Glahn et al., 2008; Ellison-Wright et al., 2008; Shenton et al., 2001; Wright et al., 2000), although some previous studies did not detect disturbances in such regions (Kanaan et al., 2005; Kubicki et al.,

Table 3
Characteristics of the subjects who underwent MRI.

		Genotype distribution of rs2230808	N	Age	Duration of illness	Drug dose (chlorpromazine equivalent)
Men	Control	*R/R*	21	39.8 ± 12.4 (20–71)		
		K carrier	26	38.9 ± 11.9 (25–69)		
		All	47	39.3 ± 12.0 (20–71)		
	Schizophrenia	*R/R*	16	44.7 ± 16.7 (22–76)	21.0 ± 16.9	770.0 ± 636.0
		K carrier	33	43.7 ± 13.0 (27–72)	21.7 ± 12.9	1183.6 ± 945.7
Women	Control	*R/R*	39	48.2 ± 13.5 (25–74)		
		K carrier	53	39.9 ± 11.6 (22–71)		
		All	92	43.4 ± 13.0 (22–74)		
	Schizophrenia	*R/R*	16	47.5 ± 12.3 (22–67)	17.2 ± 13.2	691.6 ± 566.3
		K carrier	21	46.3 ± 15.0 (23–75)	19.0 ± 13.2	731.2 ± 623.9